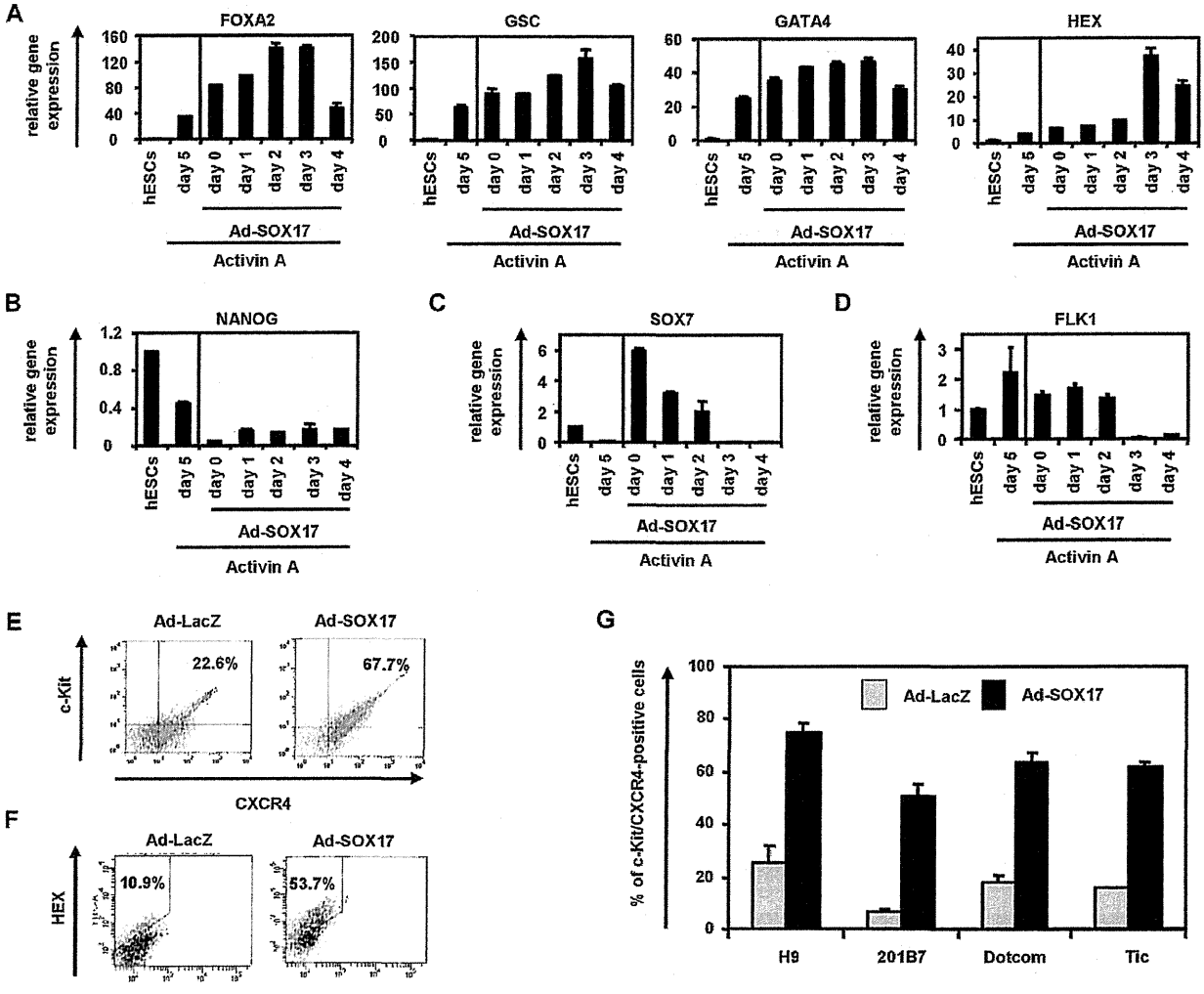

Figure 2. Efficient DE differentiation from human ESC- and iPSC-derived mesendoderm cells by SOX17 transduction. (A–D) Undifferentiated human ESCs (H9) and Activin A-induced human ESC-derived cells, which were cultured with the medium containing Activin A (100 ng/ml) for 0, 1, 2, 3, and 4 days, were transduced with 3,000 VP/cell of Ad-SOX17 for 1.5 h. Ad-SOX17-transduced cells were cultured with 100 ng/ml of Activin A, and the gene expression levels of (A) the DE markers (FOXA2, GSC, and GATA4) and anterior DE marker (HEX), (B) the pluripotent marker (NANOG), (C) the ExEn marker (SOX7), and (D) the mesoderm marker (FLK1) were examined by real-time RT-PCR on day 5 of differentiation. The horizontal axis represents the day on which the cells were transduced with Ad-SOX17. The expression levels of human ESCs on day 0 were defined 1.0. (E, F) After human ESCs were cultured with 100 ng/ml of Activin A for 3 days, human ESC-derived mesendoderm cells were transduced with Ad-LacZ or Ad-SOX17 and cultured until day 5. Ad-LacZ- or Ad-SOX17-transduced DE cells were subjected to immunostaining with anti-c-Kit, anti-CXCR4 (E) and anti-HEX antibodies (F) and then analyzed by flow cytometry. (G) After Ad-LacZ or Ad-SOX17 transduction, the DE differentiation efficacies of the human ES cell line (H9) and three human iPS cell lines (201B7, Dotcom, and Tic) were compared at day 5 of differentiation. All data are represented as the means±SD ($n=3$).
doi:10.1371/journal.pone.0021780.g002

examined hepatic gene and protein expression levels on day18 of differentiation. For this purpose, we used a human ES cell line (H9) and three human iPS cell lines (201B7, Dotcom, Tic). On day 18 of differentiation, the gene and protein expression analysis showed up-regulation of the hepatic markers albumin (ALB) [27], cytochrome P450 2D6 (CYP2D6), CYP3A4, and CYP7A1 [28] mRNA and ALB, CYP2D6, CYP3A4, CYP7A1, and cytokeratin (CK)18 proteins in both Ad-SOX17- and Ad-HEX-transduced cells transduced cells as compared with both Ad-LacZ- and Ad-HEX-transduced cells (Figures 4A and 4B). These results indicated that Ad-SOX17-transduced cells were more committed to the hepatic lineage than non-transduced cells.

Discussion

The directed differentiation from human ESCs and iPSCs is a useful model system for studying mammalian development as well as a powerful tool for regenerative medicine [29]. In the present study, we elucidated the bidirectional role of SOX17 on either ExEn or DE differentiation from human ESCs and iPSCs. We initially confirmed that initiation of SOX17 expression was consistent with the time period of PrE or mesendoderm cells formation (Figures S1 and S2). We speculated that stage-specific transient SOX17 transduction in PrE or mesendoderm could enhance ExEn or DE differentiation from human ESCs and iPSCs, respectively.

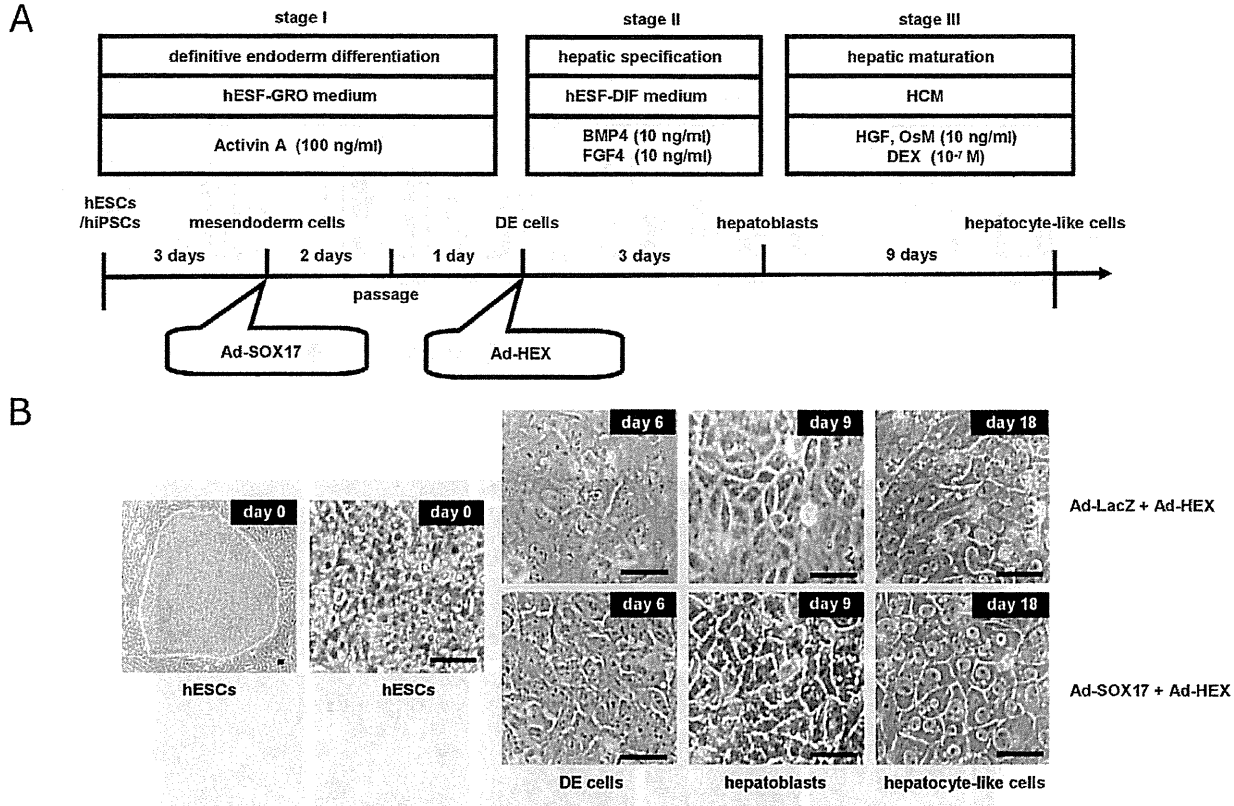

Figure 3. Hepatic Differentiation of Human ESC- and iPSC-Derived DE Cells Transduced with Ad-HEX. (A) The procedure for differentiation of human ESCs and iPSCs into hepatoblasts and hepatocyte-like cells is presented schematically. Both hESF-GRO and hESF-DIF medium were supplemented with 5 factors and 0.5 mg/ml fatty acid-free BSA, as described in the Materials and Methods section. (B) Sequential morphological changes (day 0–18) of human ESCs (H9) differentiated into hepatocyte-like cells via the DE cells and the hepatoblasts are shown. The scale bar represents 50 μm.
doi:10.1371/journal.pone.0021780.g003

SOX17 transduction at the pluripotent stage promoted random differentiation giving heterogeneous populations containing both ExEn and DE cells were obtained (Figures 2A–2C). Qu et al. reported that SOX17 promotes random differentiation of mouse ESCs into PrE cells and DE cells *in vitro* [30], which is in consistent with the present study. Previously, Niakan et al. and Seguin et al. respectively demonstrated that ESCs could promote either ExEn or DE differentiation by stable SOX17 expression, respectively [10,12]. Although these discrepancies might be attributable to differences in the species used in the experiments (i.e., human versus mice), SOX17 might have distinct functions according to the appropriate differentiation stage. To elucidate these discrepancies, we examined the stage-specific roles of SOX17 in the present study, and found that human ESCs and iPSCs could differentiate into either ExEn or DE cells when SOX17 was overexpressed at the PrE or mesendoderm stage, respectively, but not when it was overexpressed at the pluripotent stage (Figures 1 and 2). This is because endogenous SOX17 is strongly expressed in the PrE and primitive streak tissues but only slightly expressed in the inner cell mass, our system might adequately reflect the early embryogenesis [14,31].

In ExEn differentiation from human ESCs, stage-specific SOX17 overexpression in human ESC-derived PrE cells promoted efficient ExEn differentiation and repressed trophectoderm differentiation (Figures 1A and 1B), although SOX17 transduction at the pluripotent stage did not induce the efficient differentiation of ExEn cells. In our protocol, the stage-specific overexpression of SOX17 could elevate the efficacy of AFP-positive or SOX7-positive ExEn differentiation from human ESCs and iPSCs. The reason for the efficient ExEn differentiation by SOX17 transduction might be due to the fact that SOX17 lies downstream from GATA6 and directly regulates the expression of GATA4 and GATA6 [12]. Although it was previously been reported that Sox17 plays a substantial role in late-stage differentiation of ExEn cells *in vitro* [32], those reports utilized embryoid body formation, in which other types of cells, including endoderm, mesoderm, and ectoderm cells, might have influences on cellular differentiation. The present study showed the role of SOX17 in a homogeneous differentiation system by utilizing a mono-layer culture system.

In DE differentiation from human ESCs, we found that DE cells were efficiently differentiated from the human ESC-derived mesendoderm cells by stage-specific SOX17 overexpression (Figure 2). Therefore, we concluded that SOX17 plays a significant role in the differentiation of mesendoderm cells to DE cells. Although SOX17 overexpression before the formation of mesendoderm cells did not affect mesoderm differentiation, SOX17 transduction at the mesendoderm stage selectively promoted DE differentiation and repressed mesoderm differentiation (Figures 2A and 2D). These results show that SOX17 plays a crucial role in decision of DE differentiation from mesendoderm cells, as previous studies suggested [33,34]. Interestingly, SOX17 transduction at the pluripotent stage promoted not only DE

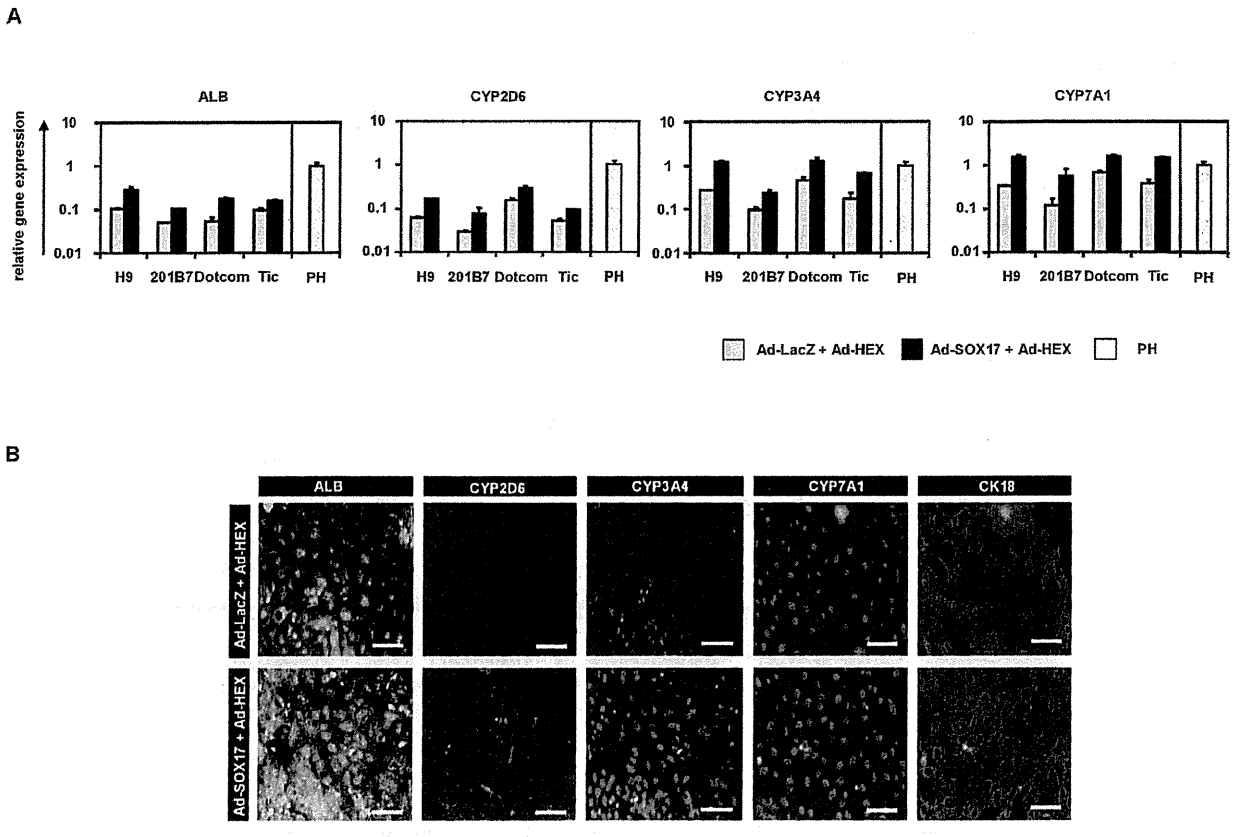

Figure 4. Characterization of hepatocyte-like cells from human ESC- and iPSC-derived DE cells. (A) The Ad-LacZ-transduced cells and Ad-SOX17-transduced cells were transduced with 3,000 VP/cell of Ad-HEX for 1.5 h on day 6. On day 18 of differentiation, the levels of expression of the hepatocyte markers (ALB, CYP2D6, CYP3A4, and CYP7A1) were examined by real-time RT-PCR in human ESC (H9)-derived hepatocyte-like cells and human iPSC (201B7, Dotcom, or Tic)-derived hepatocyte-like cells. The gene expression profiles of cells transduced with both Ad-SOX17 and Ad-HEX (black bar) were compared with those of cells transduced with both Ad-LacZ and Ad-HEX (gray bar). The expression level of primary human hepatocytes (PH, hatched bar), which were cultured 48 h after plating the cells, were defined as 1.0. All data are represented as the means±SD ($n = 3$). (B) The expression of the hepatocyte markers ALB (green), CYP2D6 (red), CYP3A4 (red), CYP7A1 (red), and CK18 (green) was also examined by immunohistochemistry on day 18 of differentiation. Nuclei were counterstained with DAPI (blue). The scale bar represents 50 μm.
doi:10.1371/journal.pone.0021780.g004

differentiation but also ExEn differentiation even in the presence of Activin A (Figures 2A and 2C), demonstrating that transduction at an inappropriate stage of differentiation prevents directed differentiation. These results suggest that stage-specific SOX17 transduction mimicking the gene expression pattern in embryogenesis could selectively promote DE differentiation.

Another important finding about DE differentiation is that the protocol in the present study was sufficient for nearly homogeneous DE and anterior DE differentiation by mesendoderm stage-specific SOX17 overexpression; the differentiation efficacies of c-Kit/CXCR4-double-positive DE cells and HEX-positive anterior DE cells were approximately 70% and 54%, respectively (Figures 2E and 2F). The conventional differentiation protocols without gene transfer were not sufficient for homogenous DE and anterior DE differentiation; the differentiation efficacies of DE and anterior DE were approximately 30% and 10%, respectively [10,11,23]. One of the reasons for the efficient DE differentiation by SOX17 transduction might be the activation of the FOXA2 gene which could regulate many endoderm-associated genes [35]. Moreover, SOX17-transduced cells were more committed to the hepatic lineage (Figure 4). This might be because the number of HEX-positive anterior DE cell populations was increased by SOX17 transduction. Recent studies have shown that the conditional expression of Sox17 in the pancreas at E12.5, when it is not normally expressed, is sufficient to promote biliary differentiation at the expense of endocrine cells [36]. Therefore, we reconfirmed that our protocol in which SOX17 was transiently transduced at the appropriate stage of differentiation was useful for DE and hepatic differentiation from human ESCs and iPSCs.

Using human iPSCs as well as human ESCs, we confirmed that stage-specific overexpression of SOX17 could promote directive differentiation of either ExEn or DE cells (Figures 1F, 2G, and 4A). Interestingly, a difference of DE and hepatic differentiation efficacy among human iPS cell lines was observed (Figures 1F and 2G). Therefore, it would be necessary to select a human iPS cell line that is suitable for hepatic differentiation in the case of medical applications, such as liver transplantation.

To control cellular differentiation mimicking embryogenesis, we employed Ad vectors, which are one of the most efficient transient gene delivery vehicles and have been widely used in both experimental studies and clinical trials [37]. Recently, we have also demonstrated that ectopic HEX expression by Ad vectors in human ESC-derived DE cells markedly enhances the hepatic differentiation [13]. Thus, Ad vector-mediated transient gene

transfer should be a powerful tool for regulating cellular differentiation.

In summary, the findings presented here demonstrate a stage-specific role of SOX17 in the ExEn and DE differentiation from human ESCs and iPSCs (Figure S8). Although previous reports showed that SOX17 overexpression in ESCs leads to differentiation of either ExEn or DE cells, we established a novel method to promote directive differentiation by SOX17 transduction. Because we utilized a stage-specific overexpression system, our findings provide further evidence that the lineage commitment in this method seems to reflects what is observed in embryonic development. In the present study, both human ESCs and iPSCs (3 lines) were used and all cell lines showed efficient ExEn or DE differentiation, indicating that our novel protocol is a powerful tool for efficient and cell line-independent endoderm differentiation. Moreover, the establishing methods for efficient hepatic differentiation by sequential SOX17 and HEX transduction would be useful for *in vitro* applications such as screening of pharmacological compounds as well as for regenerative therapy.

Materials and Methods

In vitro Differentiation

Before the initiation of cellular differentiation, the medium of human ESCs and iPSCs was exchanged for a defined serum-free medium hESF9 [38] and cultured as we previously reported. hESF9 consists of hESF-GRO medium (Cell Science & Technology Institute) supplemented with 5 factors (10 μg/ml human recombinant insulin, 5 μg/ml human apotransferrin, 10 μM 2-mercaptoethanol, 10 μM ethanolamine, and 10 μM sodium selenite), oleic acid conjugated with fatty acid free bovine albumin, 10 ng/ml FGF2, and 100 ng/ml heparin (all from Sigma).

To induce, ExEn cells, human ESCs and iPSCs were cultured for 5 days on a gelatin-coated plate in mouse embryonic conditioned-medium supplemented with 20 ng/ml BMP4 (R&D system) and 1% FCS (GIBCO-BRL).

The differentiation protocol for induction of DE cells, hepatoblasts, and hepatocyte-like cells was based on our previous report with some modifications [13]. Briefly, in DE differentiation, human ESCs and iPSCs were cultured for 5 days on a Matrigel (BD)-coated plate in hESF-DIF medium (Cell Science & Technology Institute) supplemented with the above-described 5 factors, 0.5 mg/ml BSA, and 100 ng/ml Activin A (R&D Systems). For induction of hepatoblasts, the DE cells were transduced with 3,000 VP/cell of Ad-HEX for 1.5 h and cultured in hESF-DIF (Cell Science & Technology Institute) medium supplemented with the above-described 5 factors, 0.5 mg/ml BSA, 10 ng/ml bone morphology protein 4 (BMP4) (R&D Systems), and 10 ng/ml FGF4 (R&D systems). In hepatic differentiation, the cells were cultured in hepatocyte culture medium (HCM) supplemented with SingleQuots (Lonza), 10 ng/ml hepatocyte growth factor (HGF) (R&D Systems), 10 ng/ml Oncostatin M (OsM) (R&D Systems), and 10^{-7} M dexamethasone (DEX) (Sigma).

Human ESC and iPSC Culture

A human ES cell line, H9 (WiCell Research Institute), was maintained on a feeder layer of mitomycin C-treated mouse embryonic fibroblasts (Millipore) with Repro Stem (Repro CELL), supplemented with 5 ng/ml fibroblast growth factor 2 (FGF2) (Sigma). Human ESCs were dissociated with 0.1 mg/ml dispase (Roche Diagnostics) into small clumps, and subcultured every 4 or 5 days. Two human iPS cell lines generated from the human embryonic lung fibroblast cell line MCR5 were provided from the JCRB Cell Bank (Tic, JCRB Number: JCRB1331; and Dotcom, JCRB Number: JCRB1327) [39,40]. These human iPS cell lines were maintained on a feeder layer of mitomycin C-treated mouse embryonic fibroblasts with iPSellon (Cardio), supplemented with 10 ng /ml FGF2. Another human iPS cell line, 201B7, generated from human dermal fibroblasts (HDF) was kindly provided by Dr. S. Yamanaka (Kyoto University) [6]. The human iPS cell line 201B7 was maintained on a feeder layer of mitomycin C-treated mouse embryonic fibroblasts with Repro Stem (Repro CELL), supplemented with 5 ng/ml FGF2 (Sigma). Human iPSCs were dissociated with 0.1 mg/ml dispase (Roche Diagnostics) into small clumps, and subcultured every 5 or 6 days.

Adenovirus (Ad) Vectors

Ad vectors were constructed by an improved *in vitro* ligation method [41,42]. The human SOX17 gene (accession number NM_022454) was amplified by PCR using primers designed to incorporate the 5′ BamHI and 3′ XbaI restriction enzyme sites: Fwd 5′-gcagggatccagcgccatgagcagcccgg-3′ and Rev 5′-cttctagagatcagggacctgtcacacgtc-3′. The human SOX17 gene was inserted into pcDNA3 (Invitrogen), resulting in pcDNA-SOX17, and then the human SOX17 gene was inserted into pHMEF5 [15], which contains the human EF-1α promoter, resulting in pHMEF-SOX17. The pHMEF-SOX17 was digested with I-CeuI/PI-SceI and ligated into I-CeuI/PI-SceI-digested pAdHM41-K7 [16], resulting in pAd-SOX17. The human elongation factor-1α (EF-1α) promoter-driven LacZ- or HEX-expressing Ad vectors, Ad-LacZ or Ad-HEX, were constructed previously. [13,43]. Ad-SOX17, Ad-HEX, and Ad-LacZ, which contain a stretch of lysine residue (K7) peptides in the C-terminal region of the fiber knob for more efficient transduction of human ESCs, iPSCs, and DE cells, were generated and purified as described previously [13,15,43]. The vector particle (VP) titer was determined by using a spectrophotometric method [44].

Flow Cytometry

Single-cell suspensions of human ESCs, iPSCs, and their derivatives were fixed with methanol at 4°C for 20 min, then incubated with the primary antibody, followed by the secondary antibody. Flow cytometry analysis was performed using a FACS LSR Fortessa flow cytometer (Becton Dickinson).

RNA Isolation and Reverse Transcription-Polymerase Chain Reaction (RT-PCR)

Total RNA was isolated from human ESCs, iPSCs, and their derivatives using ISOGENE (Nippon Gene) according to the manufacture's instructions. Primary human hepatocytes were purchased from CellzDirect. cDNA was synthesized using 500 ng of total RNA with a Superscript VILO cDNA synthesis kit (Invitrogen). Real-time RT-PCR was performed with Taqman gene expression assays (Applied Biosystems) or SYBR Premix Ex Taq (TaKaRa) using an ABI PRISM 7000 Sequence Detector (Applied Biosystems). Relative quantification was performed against a standard curve and the values were normalized against the input determined for the housekeeping gene, glyceraldehyde 3-phosphate dehydrogenase (GAPDH). The primer sequences used in this study are described in Table S1.

Immunohistochemistry

The cells were fixed with methanol or 4% PFA. After blocking with PBS containing 2% BSA and 0.2% Triton X-100 (Sigma), the cells were incubated with primary antibody at 4°C for 16 h, followed by incubation with a secondary antibody that was labeled

with Alexa Fluor 488 or Alexa Fluor 594 (Invitrogen) at room temperature for 1 h. All the antibodies are listed in Table S2.

Crystal Violet Staining

The human ESC-derived cells that had adhered to the wells were stained with 200 µl of 0.3% crystal violet solution at room temperature for 15 min. Excess crystal violet was then removed and the wells were washed three times. Fixed crystal violet was solubilized in 200 µl of 100% ethanol at room temperature for 15 min. Cell viability was estimated by measuring the absorbance at 595 nm of each well using a microtiter plate reader (Sunrise, Tecan).

LacZ Assay

The human ESC- and iPSC-derived cells were transduced with Ad-LacZ at 3,000 VP/cell for 1.5 h. After culturing for the indicated number of days, 5-bromo-4-chloro-3-indolyl β-D-galactopyranoside (X-Gal) staining was performed as described previously [15].

Supporting Information

Table S1 List of Taqman probes and primers used in this study.
(DOC)

Table S2 List of antibodies used in this study.
(DOC)

Figure S1 PrE cells formation from human ESCs on day 1 of differentiation. (A) The procedure for differentiation of human ESCs and iPSCs to ExEn cells by treatment with BMP4 (20 ng/ml) is presented schematically. (B) Human ESCs (H9) were morphologically changed during ExEn differentiation; when human ESCs were cultured with the medium containing BMP4 (20 ng/ml) for 5 days, the cells began to show flattened epithelial morphology. The scale bar represents 50 µm. (C–E) The tTemporal protein expression analysis during ExEn differentiation was performed by immunohistochemistry. The PrE markers COUP-TF1 [21] (red), SOX17 [14] (red), and SOX7 [14] (red) were detected on day 1. In contrast to the PS markers, the expression of the DE marker GSC [22] (red) was not detected and the level of the pluripotent marker NANOG (green) declined between day 0 and day 1. Nuclei were counterstained with DAPI (blue). The scale bar represents 50 µm.
(PDF)

Figure S2 Mesendoderm cells formation from human ESCs on day 3 of differentiation. (A) The procedure for differentiation of human ESCs and iPSCs to DE cells by treatment with Activin A (100 ng/ml) is presented schematically. hESF-GRO medium was supplemented with 5 factors and 0.5 mg/ml fatty acid free BSA, as described in the Materials and Methods. (B) Human ESCs (H9) were morphologically changed during DE differentiation; when human ESCs were cultured with the medium containing Activin A (100 ng/ml) for 5 days, the morphology of the cells began to show visible cell-cell boundaries. The scale bar represents 50 µm. (C–E) The tTemporal protein expression analysis during DE differentiation was performed by immunohistochemistry. The anterior PS markers FOXA2 [21] (red), GSC [22] (red), and SOX17 [14] (red) were adequately detected on day 3. The PS marker T [45] (red) was detected until day 3. In contrast to the PS markers, the expression of the pluripotent marker NANOG [24] (green) declined between day 2 and day 3. Nuclei were counterstained with DAPI (blue). The scale bar represents 50 µm.
(PDF)

Figure S3 Overexpression of SOX17 mRNA in human ESC (H9)-derived PS cells by Ad-SOX17 transduction. Human ESC-derived PS cells (day 1) were transduced with 3,000VP/cell of Ad-SOX17 for 1.5 h. On day 3 of differentiation, real-time RT-PCR analysis of the SOX17 expression was performed in Ad-LacZ-transduced cells and Ad-SOX17-transduced cells. On the y axis, the expression levels of undifferentiated human ESCs on day 0 was were taken defined as 1.0. All data are represented as the means±SD ($n = 3$).
(PDF)

Figure S4 Efficient transduction in Activin A-induced human ESC (H9)-derived cells by using a fiber-modified Ad vector containing the EF-1α promoter. Undifferentiated human ESCs and Activin A-induced human ESC-derived cells, which were cultured with the medium containing Activin A (100 ng/ml) for 0, 1, 2, 3, and 4 days, were transduced with 3,000 vector particles (VP)/cell of Ad-LacZ for 1.5 h. The day after transduction, X-gal staining was performed. The scale bar represents 100 µm. Similar results were obtained in two independent experiments.
(PDF)

Figure S5 Optimization of the time period for Ad-SOX17 transduction to promote DE differentiation from human iPSCs (Tic). Undifferentiated human iPSCs and Activin A-induced human iPSC-derived cells, which were cultured with the medium containing Activin A (100 ng/ml) for 0, 1, 2, 3, and 4 days, were transduced with 3,000 VP/cell of Ad-SOX17 for 1.5 h. Ad-SOX17-transduced cells were cultured with Activin A (100 ng/ml) until day 5, and then real-time RT-PCR analysis was performed. The horizontal axis represents the day on which the cells were transduced with Ad-SOX17. On the y axis, the expression levels of undifferentiated cells on day 0 was were taken defined as 1.0. All data are represented as the means±SD ($n = 3$).
(PDF)

Figure S6 Time course of LacZ expression in human ESC (H9)-derived mesendoderm cells transduced with Ad-LacZ. The hHuman ESC-derived mesendoderm cells (day 3) were transduced with 3,000 VP/cell of Ad-LacZ for 1.5 h. On days 4, 5, 6, 8, and 10, X-gal staining was performed. Note that human ESC-derived cells were passaged on day 5. The scale bar represents 100 µm. Similar results were obtained in two independent experiments.
(PDF)

Figure S7 Optimization of the time period for Ad-SOX17 transduction into Activin A-induced human ESC (H9)-derived cells. Undifferentiated human ESCs and Activin A-induced hESC-derived cells, which were cultured with the medium containing Activin A (100 ng/ml) for 0, 1, 2, 3, and 4 days, were transduced with 3,000 VP/cell of Ad-LacZ or Ad-SOX17 for 1.5 h. Ad-SOX17-transduced cells were cultured with Activin A (100 ng/ml) until day 5, then the cell viability was evaluated with crystal violet staining. The horizontal axis represents the day on which the cells were transduced with Ad-SOX17. On the y axis, the level of non-transduced cells was taken defined as 1.0. All data are represented as the means±SD (n = 3).
(PDF)

Figure S8 Model of differentiation of human ESCs and iPSCs into ExEn and DE cells by stage-specific SOX17 transduction. The ExEn and DE differentiation process is divided into at least two stages. In the first stage, human ESCs differentiate into either PrE cells by treatment with BMP4 (20 ng/ml) or mesendoderm cells by treatment with Activin A (100 ng/

ml). In the second stage, SOX17 promotes the further differentiation of each precursor cell into ExEn and DE cells, respectively. We have demonstrated that the efficient differentiation of these two distinct endoderm lineages is accomplished by stage-specific SOX17 transduction.
(PDF)

Acknowledgments

We thank Hiroko Matsumura and Misae Nishijima for their excellent technical support. We thank Mr. David Bennett and Ms. Ong Tyng Tyng for critical reading of the manuscript.

Author Contributions

Conceived and designed the experiments: K. Takayama MI K. Kawabata MFK HM. Performed the experiments: K. Takayama MI K. Tashiro. Analyzed the data: K. Takayama MI K. Kawabata K. Tashiro K. Katayama FS HM. Contributed reagents/materials/analysis tools: K. Kawabata K. Katayama FS TH MFK HM. Wrote the paper: K. Takayama K. Kawabata HM.

References

1. Enders AC, Given RL, Schlafke S (1978) Differentiation and migration of endoderm in the rat and mouse at implantation. Anat Rec 190: 65–77.
2. Gardner RL (1983) Origin and differentiation of extraembryonic tissues in the mouse. Int Rev Exp Pathol 24: 63-133.
3. Grapin-Botton A, Constam D (2007) Evolution of the mechanisms and molecular control of endoderm formation. Mech Dev 124: 253-278.
4. Tam PP. Kanai-Azuma M, Kanai Y (2003) Early endoderm development in vertebrates: lineage differentiation and morphogenetic function. Curr Opin Genet Dev 13: 393-400.
5. Thomson JA, Itskovitz-Eldor J, Shapiro SS, Waknitz MA, Swiergiel JJ, et al. (1998) Embryonic stem cell lines derived from human blastocysts. Science 282: 1145 1147.
6. Takahashi K, Tanabe K, Ohnuki M, Narita M, Ichisaka T, et al. (2007) Induction of pluripotent stem cells from adult human fibroblasts by defined factors. Cell 131: 861-872.
7. Yu J, Vodyanik MA, Smuga-Otto K, Antosiewicz-Bourget J, Frane JL, et al. (2007) Induced pluripotent stem cell lines derived from human somatic cells. Science 318: 1917--1920.
8. Xu RH, Chen X, Li DS, Li R, Addicks GC, et al. (2002) BMP4 initiates human embryonic stem cell differentiation to trophoblast. Nat Biotechnol 20: 1261--1264.
9. Pera MF. Andrade J, Houssami S, Reubinoff B, Trounson A, et al. (2004) Regulation of human embryonic stem cell differentiation by BMP-2 and its antagonist noggin. J Cell Sci 117: 1269 1280.
10. Seguin CA, Draper JS, Nagy A, Rossant J (2008) Establishment of endoderm progenitors by SOX transcription factor expression in human embryonic stem cells. Cell Stem Cell 3: 182 195.
11. Gouon-Evans V, Boussemart L, Gadue P. Nierhoff D, Koehler CI, et al. (2006) BMP-4 is required for hepatic specification of mouse embryonic stem cell-derived definitive endoderm. Nat Biotechnol 24: 1402 1411.
12. Niakan KK, Ji H, Maehr R, Vokes SA, Rodolfa KT, et al. (2010) Sox17 promotes differentiation in mouse embryonic stem cells by directly regulating extraembryonic gene expression and indirectly antagonizing self-renewal. Genes Dev 24: 312 326.
13. Inamura M, Kawabata K, Takayama K, Tashiro K, Sakurai F, et al. (2011) Efficient Generation of Hepatoblasts From Human ES Cells and iPS Cells by Transient Overexpression of Homeobox Gene HEX. Mol Ther 19: 400-407.
14. Kanai-Azuma M, Kanai Y. Gad JM, Tajima Y. Taya C, et al. (2002) Depletion of definitive gut endoderm in Sox17-null mutant mice. Development 129: 2367- 2379.
15. Kawabata K, Sakurai F. Yamaguchi T. Hayakawa T, Mizuguchi H (2005) Efficient gene transfer into mouse embryonic stem cells with adenovirus vectors. Mol Ther 12: 547- 554.
16. Koizumi N, Mizuguchi H, Utoguchi N, Watanabe Y. Hayakawa T (2003) Generation of fiber-modified adenovirus vectors containing heterologous peptides in both the HI loop and C terminus of the fiber knob. J Gene Med 5: 267-276.
17. Fujikura J, Yamato E, Yonemura S, Hosoda K, Masui S, et al. (2002) Differentiation of embryonic stem cells is induced by GATA factors. Genes Dev 16: 784- 789.
18. Koutsourakis M, Langeveld A, Patient R. Beddington R. Grosveld F (1999) The transcription factor GATA6 is essential for early extraembryonic development. Development 126: 723 732.
19. Morrisey EE. Tang Z, Sigrist K, Lu MM, Jiang F. et al. (1998) GATA6 regulates HNF4 and is required for differentiation of visceral endoderm in the mouse embryo. Genes Dev 12: 3579- 3590.
20. Kunath T. Strumpf D. Rossant J (2004) Early trophoblast determination and stem cell maintenance in the mouse- a review. Placenta 25 Suppl A: S32 38.
21. Sasaki H. Hogan BL (1993) Differential expression of multiple fork head related genes during gastrulation and axial pattern formation in the mouse embryo. Development 118: 47 59.
22. Blum M. Gaunt SJ, Cho KW. Steinbeisser H. Blumberg B. et al. (1992) Gastrulation in the mouse: the role of the homeobox gene goosecoid. Cell 69: 1097 1106.
23. Morrison GM, Oikonomopoulou I, Migueles RP. Soneji S, Livigni A, et al. (2008) Anterior definitive endoderm from ESCs reveals a role for FGF signaling. Cell Stem Cell 3: 402-415.
24. Mitsui K, Tokuzawa Y, Itoh H, Segawa K. Murakami M, et al. (2003) The homeoprotein Nanog is required for maintenance of pluripotency in mouse epiblast and ES cells. Cell 113: 631–642.
25. Shalaby F, Rossant J, Yamaguchi TP, Gertsenstein M, Wu XF, et al. (1995) Failure of blood-island formation and vasculogenesis in Flk-1-deficient mice. Nature 376: 62–66.
26. D'Amour KA, Agulnick AD, Eliazer S, Kelly OG, Kroon E, et al. (2005) Efficient differentiation of human embryonic stem cells to definitive endoderm. Nat Biotechnol 23: 1534- 1541.
27. Shiojiri N (1984) The origin of intrahepatic bile duct cells in the mouse. J Embryol Exp Morphol 79: 25–39.
28. Ingelman-Sundberg M, Oscarson M, McLellan RA (1999) Polymorphic human cytochrome P450 enzymes: an opportunity for individualized drug treatment. Trends Pharmacol Sci 20: 342-349.
29. Murry CE, Keller G (2008) Differentiation of embryonic stem cells to clinically relevant populations: lessons from embryonic development. Cell 132: 661–680.
30. Qu XB, Pan J, Zhang C, Huang SY (2008) Sox17 facilitates the differentiation of mouse embryonic stem cells into primitive and definitive endoderm in vitro. Dev Growth Differ 50: 585--593.
31. Sherwood RI, Jitianu C, Cleaver O, Shaywitz DA, Lamenzo JO, et al. (2007) Prospective isolation and global gene expression analysis of definitive and visceral endoderm. Dev Biol 304: 541 555.
32. Shimoda M, Kanai-Azuma M, Hara K, Miyazaki S, Kanai Y. et al. (2007) Sox17 plays a substantial role in late-stage differentiation of the extraembryonic endoderm in vitro. J Cell Sci 120: 3859- 3869.
33. Yasunaga M, Tada S, Torikai-Nishikawa S, Nakano Y, Okada M, et al. (2005) Induction and monitoring of definitive and visceral endoderm differentiation of mouse ES cells. Nat Biotechnol 23: 1542- 1550.
34. Gadue P. Huber TL, Paddison PJ, Keller GM (2006) Wnt and TGF-beta signaling are required for the induction of an in vitro model of primitive streak formation using embryonic stem cells. Proc Natl Acad Sci U S A 103: 16806- 16811.
35. Levinson-Dushnik M, Benvenisty N (1997) Involvement of hepatocyte nuclear factor 3 in endoderm differentiation of embryonic stem cells. Mol Cell Biol 17: 3817- 3822.
36. Spence JR, Lange AW. Lin SC, Kaestner KH, Lowy AM, et al. (2009) Sox17 regulates organ lineage segregation of ventral foregut progenitor cells. Dev Cell 17: 62-74.
37. Mizuguchi H, Hayakawa T (2004) Targeted adenovirus vectors. Hum Gene Ther 15: 1034--1044.
38. Furue MK, Na J, Jackson JP. Okamoto T. Jones M, et al. (2008) Heparin promotes the growth of human embryonic stem cells in a defined serum-free medium. Proc Natl Acad Sci U S A 105: 13409 13414.
39. Makino H, Toyoda M, Matsumoto K, Saito H, Nishino K, et al. (2009) Mesenchymal to embryonic incomplete transition of human cells by chimeric OCT4/3 (POU5F1) with physiological co-activator EWS. Exp Cell Res 315: 2727--2740.
40. Nagata S, Toyoda M, Yamaguchi S, Hirano K. Makino H, et al. (2009) Efficient reprogramming of human and mouse primary extra-embryonic cells to pluripotent stem cells. Genes Cells 14: 1395 1404.
41. Mizuguchi H, Kay MA (1998) Efficient construction of a recombinant adenovirus vector by an improved in vitro ligation method. Hum Gene Ther 9: 2577 2583.
42. Mizuguchi H, Kay MA (1999) A simple method for constructing E1- and E1/E4-deleted recombinant adenoviral vectors. Hum Gene Ther 10: 2013 2017.
43. Tashiro K, Kawabata K, Sakurai H. Kurachi S, Sakurai F. et al. (2008) Efficient adenovirus vector-mediated PPAR gamma gene transfer into mouse embryoid bodies promotes adipocyte differentiation. J Gene Med 10: 498 507.
44. Maizel JV, Jr.. White DO. Scharff MD (1968) The polypeptides of adenovirus. I. Evidence for multiple protein components in the virion and a comparison of types 2. 7A. and 12. Virology 36: 115 125.
45. Wilkinson DG. Bhatt S. Herrmann BG (1990) Expression pattern of the mouse T gene and its role in mesoderm formation. Nature 343: 657 659.

Journal of Chromatography A, 1218 (2011) 4772–4778

Contents lists available at ScienceDirect

Journal of Chromatography A

journal homepage: www.elsevier.com/locate/chroma

Partial-filling affinity capillary electrophoresis of glycoprotein oligosaccharides derivatized with 8-aminopyrene-1,3,6-trisulfonic acid

Sachio Yamamoto, Chikayo Shinohara, Eriko Fukushima, Kazuaki Kakehi, Takao Hayakawa, Shigeo Suzuki*

Faculty of Pharmaceutical Sciences, Kinki University, 3-4-1 Kowakae, Higashi-Osaka, Japan

ARTICLE INFO

Article history:
Received 11 January 2011
Received in revised form 15 April 2011
Accepted 17 May 2011
Available online 27 May 2011

Keywords:
Partial-filling affinity capillary electrophoresis
8-Aminopyrene-1,3,6-trisulfonic acid
Glycoprotein
Lectin
Binding constant

ABSTRACT

Partial-filling affinity capillary electrophoresis has been applied to the simultaneous analysis of interactions between glycoprotein oligosaccharides and certain plant lectins. A lectin solution and a mixture of glycoprotein-derived oligosaccharides labeled with 8-aminopyrene-1,3,6-trisulfonic acid were introduced to a neutrally coated capillary in this order, and separated by application of a negative voltage. Interaction of a lectin with each oligosaccharide in the mixture was observed as the specific retardation or dissipation of peaks, in addition to the size/charge separation of oligosaccharides by zone electrophoresis in the remainder (≈90%) of the capillary. The strength of the interaction with lectin was controlled by introducing an appropriate volume of lectin solution. Application of various specificities of lectins indicated characteristic migration profiles of the oligosaccharides. Moreover, sequential injection of four lectins (*Maachia amurensis* mitogen, *Sambucus sieboldiana* agglutinin, *Erythrina cristagalli* agglutinin, *Aleuria aurantia* lectin) induced complete dissipation of complex-type oligosaccharides and enabled specific determination of the presence of high-mannose oligosaccharides without the interference or alteration of the electropherogram in porcine thyroglobulin. This method was also applied to determine the binding constants of ovalbumin-derived oligosaccharides to wheat germ agglutinin.

1. Introduction

Capillary electrophoresis (CE) is a highly successful separation technique for the analysis of biomolecules. Capillaries with an i.d. of 50–100 μm have a high electrical resistance and a large surface area-to-volume ratio. Therefore, very high electrical fields (≈650 V/cm) can be applied. This results in short analysis times and high resolution of a mixture of closely related components in a sample.

Various separation techniques have been developed in the analysis of biochemical species. One versatile technique, affinity capillary electrophoresis (ACE), has been used to examine various interactions, including protein–drug, protein–carbohydrate, and antigen–antibody [1–5]. ACE is an analytical approach in which the change of migration patterns or times of interaction of molecules in an electrical field is recorded as the function of ligand concentration. It is used to identify specific binding and to determine binding constants. The availability and power of ACE results from four main advantages over other complementary techniques: (1) only minute quantities of sample are required; (2) the provided sample need not be pure because CE can be used to distinguish each analyte and those analytes of interest from the impurities; (3) automated CE instrumentation enhances the reliability of obtained data; and (4) molecular interactions can be characterized in free solution [6].

We previously applied this ACE technique for the profiling of oligosaccharides in glycoprotein specimens and calculation of their binding constants [7], screening of the specificity of tulip lectins [8], and characterization of milk oligosaccharides [9]. The ACE of lectins has certain advantages in the glycobiology era: (1) easy interpretation due to the combinatorial usage of lectins can provide detailed information of oligosaccharide structures; (2) high-speed analysis because the separation is completed within 30 min for a single run; and (3) high sensitivity by labeling with fluorescent tags enabling sensitive determination of the interaction. However, the method also has some disadvantages. The concentration, components and pH of the electrophoresis buffers have limited to sustain activity of the lectin used, and the usage of protein-containing buffers can complicate analyses due to adsorption of proteins to the capillary, vials and electrodes.

The use of a partial-filling method in ACE has been demonstrated to be effective for studying interactions [10]. In this technique, the capillary is filled with buffer. A "plug" of solution containing ligand

* Corresponding author. Tel.: +81 6 6721 2332; fax: +81 6 6721 2353.
E-mail address: suzuki@phar.kindai.ac.jp (S. Suzuki).

0021-9673/$ – see front matter © 2011 Elsevier B.V. All rights reserved.
doi:10.1016/j.chroma.2011.05.057

is introduced to the inlet before injection of a sample containing the receptor. A high voltage is then applied. During electrophoresis, analytes flow through the zone of the "ligand plug" (where the receptor interacts with the ligand). This method seems very attractive in lectin ACE for oligosaccharide complexes because the affinity binding zone and the separation zone based on the charge/size ratio of analytes can be readily distinguished in a capillary. Also, the contribution of these two zones to the separation profile can be easily controlled by changing the injection time of the receptor solution. However, a higher concentration of lectin is required in the partial-filling technique because the length of the lectin plug is often very small compared with that of the capillary. This may be of particular concern for the adsorption of lectin to the capillary (not to the electrodes and vials) and physical adsorption of sample components to the lectin.

In the present study, we evaluated the partial-filling ACE technique as an alternative of the previous ACE method using a lectin-added electrophoresis buffer to ascertain if the: (1) specificity of lectins was fully maintained in partial-filling mode; (2) extent of the interaction between oligosaccharides and partially filled lectin could be controlled by changing the injection time of the lectin solution; (3) reproducibility of the introduction of lectin solution was sufficiently high for the calculation of binding constants. We also applied this technique for the one-step determination of high-mannose type oligosaccharides by sequential injection of a series of lectins.

2. Materials and methods

2.1. Chemicals

8-Aminopyrene-1,3,6-trisulfonic acid (APTS), porcine thyroglobulin, human α_1-acid glycoprotein, human transferrin, and hen ovalbumin were obtained from Sigma–Aldrich Japan K.K. (Tokyo, Japan). *Aleuria aurantia* lectin (AAL), castor bean lectin (RCA_{120}), concanavalin A (Con A), *Datura stramonium* agglutinin (DSA), *Erythrina cristagalli* agglutinin (ECA), *Lens culinaris* agglutinin (LCA), *Maachia amurensis* mitogen (MAM), *Phaseolus vulgaris* agglutinin E_4 and L_4 (PHA-E_4 and PHA-L_4), pokeweed mitogen (PWM), *Sambucus sieboldiana* agglutinin (SSA), and wheat germ agglutinin (WGA) were obtained from Seikagaku Corporation (Tokyo, Japan). Peptide-N^4-(*N*-acetyl-β-D-glucosaminyl)asparagines amidase F (PNGase F, EC 3.5.1.52) was from Roche Applied Science (Tokyo, Japan). Sodium cyanoborohydride ($NaBH_3CN$) and iodoacetamide were obtained from Wako Pure Chemical Industries Limited (Osaka, Japan). Other reagents were of the highest commercial grade.

2.2. Preparation of APTS-labeled oligosaccharides

N-Linked oligosaccharides were prepared from 50 μg of lyophilized glycoprotein. A sample was dissolved in 50 μL of 50 mM phosphate buffer (pH 7.9) containing 0.1% sodium dodecyl sulfate and 2% 2-mercaptoethanol. The solution was heated at 100 °C for 5 min. After cooling, the solution was mixed with 5 μL of 7.5% NP-40 and 5 mU of recombinant PNGase F, and the reaction mixture incubated for 2 h at 37 °C. Deglycosylated proteins were precipitated by the addition of 180 μL of ice-cold ethanol and removed by centrifugation at 10,000 rpm for 5 min. The released oligosaccharides in the supernatant were dried in a centrifugal vacuum evaporator. They were labeled through reductive amination by the addition of 2 μL of 0.2 M APTS in 15% acetic acid and 2 μL of 1 M $NaBH_3CN$ in tetrahydrofuran. The labeling mixture was heated for 1 h at 80 °C. Usage of acetic acid and a higher reaction temperature causes partial loss of sialic acids from oligosaccharides. The solution was then diluted with water, and excess APTS was removed by chromatography using a Sephadex G-25 column (1 cm i.d. 30 cm) with 10 mM acetic acid as eluent. The first eluting fluorescent peak was observed at an excitation wavelength of 490 nm and an emission wavelength of 520 nm. The product was collected and evaporated to dryness. The residue was dissolved in 500 μL of water and stored in a refrigerator.

2.3. Partial-filling ACE of APTS-labeled oligosaccharides

In all CE separations, polydimethylsiloxane-coated capillaries (InertCap I®; GL Sciences Incorporated, Tokyo, Japan) of i.d. 50 μm with an effective length of 40 cm (50 cm in total) were used with 50 mM Tris–acetate buffer (pH 7.0) containing 0.8% hydroxypropylcellulose as running buffers. A P/ACE MDQ CE machine (Beckman Coulter Incorporated, Brea, CA, USA) equipped with a laser-induced fluorometric detection system was used. The capillary was thermostated at 25 °C. All lectins were dissolved in the running buffer at 1 mg/mL. A lectin solution was injected by application of a pressure of 2.07–6.9 kPa for 3–50 s; then a solution of APTS-oligosaccharides was injected for 5 s at 3.45 kPa. Separation was conducted by application of −15 kV. APTS oligosaccharides were detected by an argon laser-induced fluorometric detection with a band pass filter for fluorescein. After each run, a lectin solution in the capillary was removed by introducing buffer solution from the anodic side by pressure application (34.5 kPa, 2 min). The volume of lectin solution injected in a capillary was calculated using the method at the Internet website of the manufacturer according to the following equation [11].

$$V = \frac{\Delta P d^4 \pi t}{128 \eta L}$$

where V is the volume delivered across the capillary, ΔP denotes the pressure drop across the capillary (in Pascals), d signifies the internal diameter of the capillary (meters), t is the duration of pressure application (seconds), η represents the buffer viscosity (Pascal seconds), and L is the total capillary length (meters).

2.4. Calculation of binding constants

Migration time in the lectin plug (t_L) was calculated using the following equation.

$$t_L = (t - t_0)\frac{l_T - l_L}{l_T}$$

where t and t_0 are the migration time in the presence or absence of lectin, respectively, l_T is the effective length, and the length of the lectin plug l_L can be obtained as described in the section above. Binding constants of ovalbumin-derived oligosaccharides to WGA was calculated by *y*-reciprocal method [12] according to the following equation.

$$\frac{[L]}{\mu_p^{eff} - \mu_p^0} = \frac{1}{\mu_c^0 - \mu_p^0} \times [L] + \frac{1}{K_f(\mu_c^0 - \mu_p^0)} = f([L])$$

where $[L]$, K_f are the concentration of lectin in plug, and binding constant, respectively. μ_p^{eff}, μ_p^0, and μ_c^0 are effective electrophoretic mobility of APTS-oligosaccharide under the presence of lectin, mobility of free APTS-oligosaccharide and the mobility of APTS–WGA complex, respectively. From the linear relation in the plots of $[L]/(\mu_p^{eff} - \mu_p^0)$ versus $[L]$, we can obtain binding constants as slope/intercept.

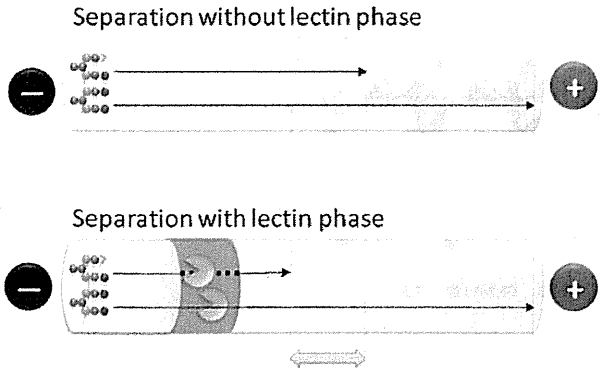

Fig. 1. Image of partial-filling affinity capillary electrophoresis of APTS-labeled oligosaccharides with lectins using a neutrally coated capillary. A specific delay indicated as an arrow (↔) indicates interaction with lectin partially filled in a capillary.

3. Results and discussion

3.1. Experimental design

Fig. 1 portrays the experimental design of partial-filling ACE. A lectin solution and then APTS-labeled oligosaccharides were introduced by hydrodynamic means to a neutrally coated capillary filled with electrophoresis buffer. Lectins with a high molecular mass had minimal electrophoretic velocity in a neutral background solution. In contrast, APTS derivatives, having three sulfonate groups, induced a high velocity in electric field. By applying a negative voltage to the capillary, APTS-labeled oligosaccharides quickly moved towards to the anode based on their size-to-charge ratio and passed through a zone of lectin solution. APTS oligosaccharides recognized by the lectin were slowed down in the lectin plug depending on affinity strength and complex mobility. The migration times were increased and often accompanied by peak broadening. In contrast, APTS oligosaccharides having no affinity for the lectin migrated with constant velocity over the capillary, and their elution profile did not change in the presence of lectin. Therefore, alteration of electrophoretic profiles in the presence of lectins directly indicated the affinity of specific oligosaccharides to the lectin.

In this experimental design, the removal of electroendoosmotic flow (EOF) and the suppression of adsorption of lectins was important. The static coating was very important for this purpose. A capillary neutrally coated with polydimethylsiloxane effectively removes EOF, and unfavorable adsorption of APTS oligosaccharides and lectins was suppressed by the addition of hydroxylpropylcellulose in the electrophoresis buffer. Moreover, to reduce analytical complications due to the adsorption of denatured lectins to the capillary, the lectin zone after each analytical run was removed from the inlet by the application of pressure to the capillary outlet. Under the optimized condition described above, the electrophoretic profiles did not change throughout this work.

3.2. Partial-filling lectin ACE of a mixture of high mannose and complex-type oligosaccharides derived from porcine thyroglobulin

In an initial series of experiments, we examined if partial-filling ACE could be used as an alternative to previous ACE using lectin-impregnated electrophoresis buffer [7]. We chose porcine thyroglobulin as an oligosaccharide pool to achieve this aim. This glycoprotein contains a series of high-mannose-type and complex-type oligosaccharides (Fig. 2(A)) [13–16]. We chose a series of lectins (MAM, DSA, PWM, PHA-L_4, SSA, LCA, ECA, WGA, Con A, AAL, and PHA-E_4) for this study. Before injection of APTS-labeled oligosaccharides, each lectin was dissolved in the running buffer at 1 mg/mL (10–30 μM), and introduced at 3.45 kPa for 30 s (which occupied 18 mm or 4.5% of the capillary to the detection window). Migrations of the oligosaccharides in the presence of lectins are shown in Fig. 2(B).

MAM is known to recognize complex-type oligosaccharides containing α2,3-linked NeuAc [17]. DSA is specific to polylactosamine and tetraantennary oligosaccharides [18]. PWM is specific to *N*-acetyllactosamine [19], and PHA-L_4 recognizes some tri- and tetraantennary oligosaccharides [20,21]. Electropherograms obtained in the presence of these lectins were approximately identical to the reference electropherogram shown at the bottom of Fig. 2(B). Thyroglobulin contains a series of biantennary complex oligosaccharides, indicating that it has no affinity for these lectins.

In contrast to the upper four traces of Fig. 2(B), ACE using other lectins as shown in the subsequent seven traces indicated affinity for thyroglobulin oligosaccharides, and showed specific migration profiles. SSA recognizes α2,6-linked NeuAc [22]. Partial-filling analysis using SSA did not alter the migration profiles of peak 4 and peaks 7–12, and indicated complete dissipation of peaks 1 to 3, 5, and 6. Disappearance of these peaks indicated the presence of α2,6-linked NeuAc. In contrast, other peaks showing identical migration times with reference data shown in the bottom trace of Fig. 2(B) did not contain α2,6-linked NeuAc. LCA has affinity for biantennary oligosaccharides with α1,6-linked Fuc in its core [23]. Severe broadening and slight retardation (*ca.* 10 s) of peaks 1 to 3, 5, and 6 implied that these peaks were assignable to the corresponding oligosaccharides. ECA shows specificity to terminal β-linked Gal residues [24]. Peak 2 and peak 5 were apparently retarded *ca.* 40 s by the addition of ECA, which implied oligosaccharides containing free Gal residues in their termini. WGA recognizes β-GlcNAc residues and also shows affinity for NeuAc-containing complex-type oligosaccharides [25]. Retardation and broadening of peaks 1 to 3, 5, and 6 were observed using WGA. Absence of terminal GlcNAc residues in thyroglobulin implied that these peaks were assignable to NeuAc-containing complex-type oligosaccharides. Con A shows strong affinity for high-mannose-type oligosaccharides and moderate affinity for biantennary complex-type oligosaccharides [26]. All oligosaccharides in thyroglobulin matched the specificity of Con A. Separation using Con A caused disappearance of most peaks. AAL is a Fuc-binding lectin; the binding strength to α1,6-linked Fuc is higher than those for α1,2-linked and α1,3-linked Fuc [27]. All complex oligosaccharides in this glycoprotein reportedly contain α1,6-linked Fuc residues, which implies that all complex-type oligosaccharides in thyroglobulin should be trapped by this lectin. The electropherogram indicated that peaks 1 to 3, 5, and 6 were recognized by AAL, and that their migration times were increased *ca.* 2 min. The peaks were assignable to complex-type oligosaccharides containing Fuc residues. PHA-E_4 recognizes biantennary oligosaccharides and triantennary oligosaccharides having two lactosamine branches at α1,3-linked Man; their affinity is reduced by the presence of terminal sialic acids [28]. From comparison of the reference electropherogram, the migration times of peaks 2, 5, and 6 were increased by ≈30 s, which indicated that these peaks were trapped by this lectin and were assignable to biantennary oligosaccharides with terminal Gal residues.

As shown above, lectins recognize specific oligosaccharides in oligosaccharide pools. The oligosaccharide peaks trapped by lectins indicate broadening of peaks and/or retardation of the migration time. By contrast, peaks of oligosaccharides with no affinity for lectins indicate an identical migration time and identical migration profile. The concentration of lectin solution in the partial-filling method was almost tenfold higher than that of our previous ACE method using lectin-impregnated electrophoresis buffer. In our previous work, we studied a conventional type of ACE of thyroglobulin oligosaccharides, and found that 10 μM of lectin induced severe tailing of peaks of excess reagent and unbound oligosac-

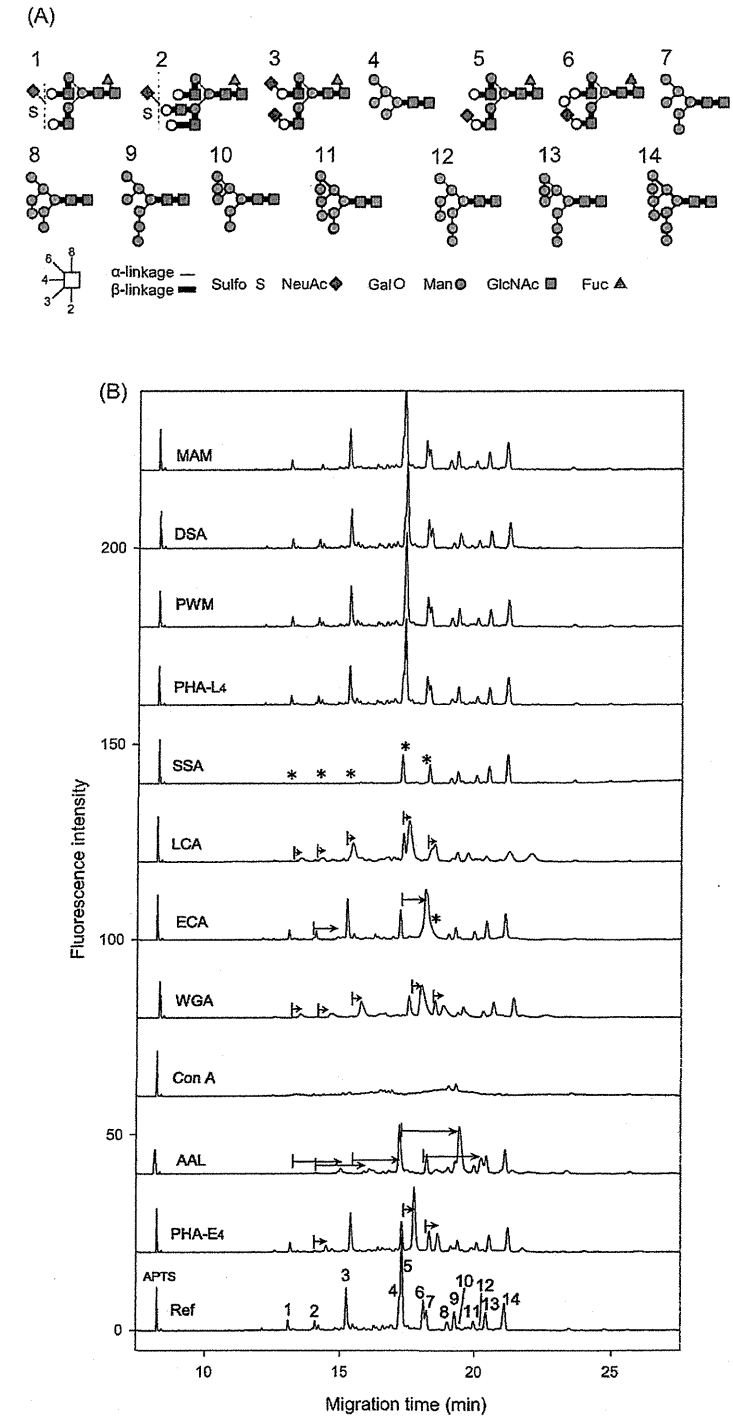

Fig. 2. Oligosaccharide structures previously reported and tentative assignment of peaks (A) and partial-filling affinity capillary electrophoresis of APTS-labeled oligosaccharides derived from porcine thyroglobulin with various lectins (B). Lectin solution (1 mg/mL, 0.25 mg/mL for Con A) was injected at 3.45 kPa for 30 s; then APTS oligosaccharides (0.1 mg/mL as glycoprotein) were injected at 3.45 kPa for 30 s. Conditions: running buffer, 50 mM Tris–acetate buffer, pH 7.0 containing 0.8% hydroxypropylcellulose; capillary, polydimethylsiloxane-coated, 50 μm i.d., 40 cm/50 cm; applied voltage, −15 kV; detection, 488 nm (excitation)/520 nm (emission).

charides [8]. In contrast, partial-filling techniques using a higher concentration of lectins indicated good separation, and did not indicate non-specific adsorption. This may be due to the separation of the affinity zone and separation zone in the partial-filling method.

3.3. *Partial-filling ACE by changing the injection volume of lectins*

As a second step, we confirmed the applicability of partial-filling ACE for various oligosaccharides derived from other glycoproteins

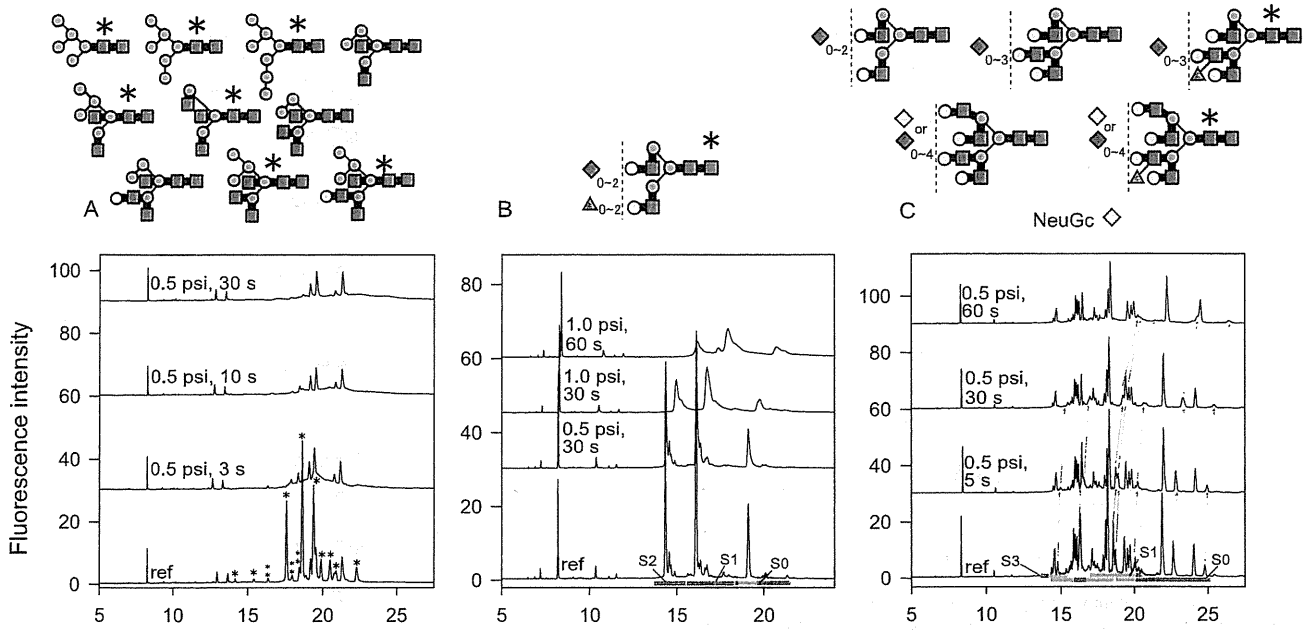

Fig. 3. Representative electropherograms of APTS-labeled oligosaccharides derived from ovalbumin with Con A (A), human transferrin with RCA_{120} (B), and α_1-acid glycoprotein with AAL (C). Lectin injection conditions are shown in each electropherogram. Gray bars with *Sx* indicate estimated elution area of trisialo-, disialo-, monosialo- and asialooligosaccharides. Other symbols and the other conditions were identical to those shown in Fig. 2. Starred oligosaccharides are expected to show affinity to the lectin.

(ovalbumin, transferrin, and α_1-acid glycoprotein) by changing the injection time of lectins. Some of the results are depicted in Fig. 3.

Ovalbumin contains a series of high mannose-type oligosaccharides ($Man_{5-7}GlcNAc_2$), a complex-type oligosaccharide ($Man_3GlcNAc_5$), and some hybrid-type oligosaccharides with bisecting GlcNAc ($Man_{4-5}GlcNAc_{5-6}Gal_{0-1}$) [29,30]. Fig. 3(A) shows selected electropherograms obtained by changing the injection time of Con A. Peaks with a single asterisk disappeared after injection of 0.25 mg/mL of Con A at 3.45 kPa for 3 s (although retardation was not observed). In contrast, some peaks with two asterisks slightly broadened, and injection at 3.45 kPa and 30 s was needed for complete dissipation. Four other unmarked peaks that appeared at 19.2, 19.5, 20.8, and 21.3 were not altered by injection of Con A. According to the binding specificity of Con A, hybrid-type oligosaccharides with non-branched oligomannosyl sequences may not have affinity for Con A. Peak dissipation without retardation indicated that the recognition of oligosaccharides in the plug of Con A was fast but that dissociation of the oligosaccharide–Con A complex was kinetically very slow. This phenomenon is not specific for the partial-filling method; our previous work also indicated the dissipation profiles in affinity electrophoresis using electrophoretic buffer containing Con A [7].

Fig. 3(B) shows the change in migration of transferrin oligosaccharides by changing the injection times of RCA_{120}. This glycoprotein contains mainly biantennary complex-type oligosaccharides with α2,6-linked NeuAc (some of which also contain α1,6-linked Fuc in core chitobiose and/or α1-3-linked Fuc in terminal lactosamine residues). We applied drastic conditions for APTS labeling, which caused partial loss of sialic acids. As shown in the lower part of Fig. 3(B), tall peaks corresponding to disialo-, monosialo- and asialooligosaccharides appeared at 14.3, 16.1, and 19.1 min, respectively. Small peaks following major peaks therefore corresponded to fucosylated oligosaccharides. Injection of RCA_{120} lectin induced severe tailing and broadening of all transferrin peaks. Moreover, the long period of injection of this lectin induced slight retardation of migration.

Human α_1-acid glycoprotein contains bi-, tri-, and tetraantennary complex-type oligosaccharides. Some triantennary and tetraantennary oligosaccharides have α1,3-linked Fuc at a lactosamine branch; their non-reducing ends are terminated with NeuAc and NeuGc [31]. Therefore, the oligosaccharide mixture has very complicated electropherograms. For partial-filling analysis using a Fuc-specific lectin, AAL is depicted in Fig. 3(C). The Fuc-containing peaks are distributed irregularly throughout the electropherogram; some peaks with asterisks are gradually broadened and retarded along with the increase of injection time of AAL.

An advantage of partial-filling ACE can be seen by changing the effective plug length of the lectin solution without varying the concentration of the components. This feature enhances the applicability of this method.

3.4. Multiple-injection analyses

Combinatorial usage of lectins having various specificities might be useful for the profiling of specific oligosaccharides in a complex mixture [32]. However, reports on the use of a lectin mixture for structural profiling of oligosaccharides are lacking because some lectins such as ECA, LCA, PHA, PWM and SSA are glycoproteins. Therefore mixing of lectins including them often causes aggregation [33]. Therefore, lectin mixing is unfavorable. In our method, a combinatorial assay using a series of lectins can be realized by injecting each lectin solution sequentially into the capillary before the analysis. We chose porcine thyroglobulin as a model oligosaccharide pool and tried specific detection of high-mannose-type oligosaccharides from a pool including a series of complex-type oligosaccharides. To trap all complex-type oligosaccharides, we chose four lectins: α2,3-NeuAc-specific MAM, α2,6-NeuAc-specific SSA, β-Gal-specific ECA, and α-Fuc-specific AAL. These four lectins were injected at 3.45 kPa for 30 s in this order. Thyroglobulin oligosaccharides were then injected and separated. The separation profile is shown in the upper panel of Fig. 4 (which shows only selected peaks). Peaks observed at 12–17 min, large peaks appear-

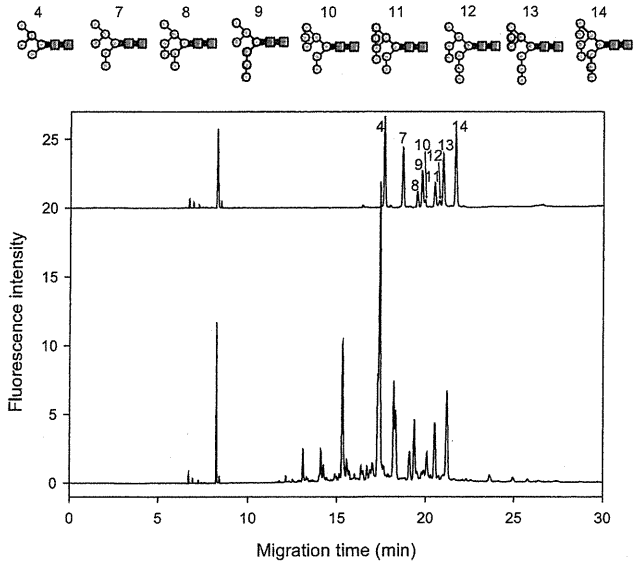

Fig. 4. Partial-filling affinity capillary electrophoresis using a series of lectins to identify high-mannose-type oligosaccharides in an oligosaccharide pool derived from porcine thyroglobulin. A 1 mg/mL solution of MAM, SSA, ECA, and AAL was introduced at 3.45 kPa for 30 s in this order; then APTS oligosaccharides from porcine thyroglobulin were injected for 5 s. The lower trace shows the reference data obtained without lectins. The other conditions were identical to those shown in Fig. 2.

ing at 17.5 min and 18.1 min, and other minor peaks appearing in reference electropherograms had disappeared completely. As shown in Fig. 2, most of the disappeared peaks were trapped by SSA. However, several minor peaks appearing at ≈15 min, 19 min, and 23–27 min, also disappeared from this profile. The same profile was also obtained by changing the injection order of the lectin solution. Moreover, the upper trace was very similar to the separation of APTS-labeled high-mannose-type oligosaccharides [34]. We speculated peaks at 17.3 min for $Man_5GlcNAc_2$, 18.2 min for $Man_6GlcNAc_2$, 19.3 min and 19.4 min for $Man_7GlcNAc_2$, 20.0 min and 20.5 min for $Man_8GlcNAc_2$, and 21.2 min for $Man_9GlcNAc_2$. This technique can be used to specifically detect oligosaccharides in a complex mixture if a suitable set of lectins is chosen.

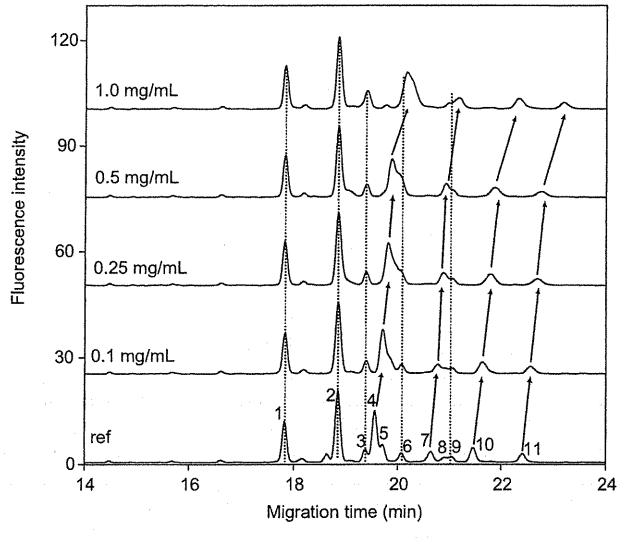

Fig. 5. Partial-filling affinity capillary electrophoresis of APTS-labeled oligosaccharides derived from ovalbumin using WGA (0, 0.1, 0.25, 0.5 and 1.0 mg/mL) for the calculation of binding constants of selected peaks. Tentative assignments of peaks are shown in Table 1. The other conditions were identical to those shown in Fig. 2.

Table 1
Tentative peak assignment and their binding constant to WGA.

Peak no.	Structure	Ka (M^{-1})
1		$<10^2$
2		$<10^2$
3		$<10^2$
4		91,000
5		ND
6		$<10^2$
7		82,000
8		ND
9		$<10^2$
10	Unknown	88,000
11		70,000

ND: not determined.

3.5. Calculation of binding constants

Calculation of binding constants is an important step in the evaluation of protein–oligosaccharide interactions, and understanding the biological significance of oligosaccharides attached to glycoproteins. ACE is important because this method is available for simultaneous analyses of the resolution of components and affinity for ligands. In the present study, we extended the use of partial-filling ACE to estimate the binding constants between WGA and APTS-labeled oligosaccharides derived from ovalbumin. These experiments were conducted by injecting an identical volume of a series of different concentrations of WGA solution. The migration times of some peaks were retarded with the increase of WGA concentration as shown in Fig. 5. Peaks 1, 2, 3, 6, and 9 did not change, but the migration times of peaks 4, 5, 7, 8, 10, and 11 increased gradually with WGA concentration. The difference in the mobilities of these peaks and concentration of WGA indicated a linear relationship in the *y*-reciprocal plots. Binding constants were obtained from the linear plot in the slope/intercept form, and the results presented in Table 1. The binding constants obtained were distributed

between 7.0×10^4 and 9.1×10^4 M^{-1}. The results obtained using the present method indicated good correlation with our previous work using lectin-immobilized silica LC [35]. Moreover, we believe that the binding constants obtained in free solution are more reliable and accurate.

4. Conclusion

Partial-filling lectin ACE can be used effectively to study the interaction between glycoprotein oligosaccharides with some plant lectins. Usage of a polydimethylsiloxane-coated capillary and hydroxypropylcellulose-impregnated electrophoretic buffer prohibits the generation of EOF and adsorption of lectins to the inner wall of the capillary. Moreover, APTS labeling enables sensitive determination of affinity profiles using minute amounts of oligosaccharides. We have shown these features of partial-filling lectin ACE by applying a series of lectins to examine affinity with a mixture of high-mannose and complex-type oligosaccharides derived from thyroglobulin, and by changing the injection conditions of lectins to selected glycoprotein oligosaccharides. Changes in electrophoretic profiles were observed as mobility shift, peak broadening, and peak disappearance. Sequential injection of a suitable set of lectins may enables detection and quantitation of specific oligosaccharides. This feature is applicable to quality control in the production of various glycoprotein pharmaceuticals, and an application will be shown near future. The method was also applied to obtain binding constants between WGA and ovalbumin oligosaccharides. Therefore, this is a convenient candidate method to detect specific oligosaccharides in glycoproteins.

Acknowledgments

This work was supported as a "High-Tech Research Center" Project for Private Universities by a matching fund subsidy from the Ministry of Education, Culture, Sports, Science and Technology (MEXT), 2007–2011.

References

[1] X. Liu, F. Dahdouh, M. Salgado, F.A. Gomez, J. Pharm. Sci. 98 (2008) 394.
[2] N.H.H. Heegaard, Electrophoresis 24 (2003) 3879.
[3] C. Bertucci, M. Bartolini, R. Gotti, V. Andrisano, J. Chromatogr. B 797 (2003) 111.
[4] Y. Tanaka, S. Terabe, J. Chromatogr. B 768 (2002) 81.
[5] R.M.G. Duijn, J. Frank, G.W.K. van Dedem, E. Baltussen, Electrophoresis 21 (2000) 3905.
[6] J. Zavaleta, D. Chinchilla, A. Brown, A. Ramirez, V. Calderon, T. Sogomonyan, F.A. Gomez, Curr. Anal. Chem. 2 (2006) 35.
[7] K. Nakajima, Y. Oda, M. Kinoshita, K. Kakehi, J. Proeome Res. 2 (2003) 81.
[8] K. Nakajima, M. Kinoshita, Y. Oda, T. Masuko, H. Kaku, N. Shibuya, K. Kakehi, Glycobiology 14 (2004) 793.
[9] K. Nakajima, M. Kinoshita, N. Matsushita, T. Urashima, M. Suzuki, A. Suzuki, K. Kakehi, Anal. Biochem. 348 (2006) 105.
[10] A. Amini, D. Westerlund, Anal. Chem. 70 (1998) 1425.
[11] http://www.beckmancoulter.com/resourcecenter/labresources/ce/ceexpert.asp.
[12] A. Varenne, P. Gareil, S. Colliec-Jouault, R. Daniel, Anal. Biochem. 315 (2003) 152.
[13] P. deWaard, A. Koorevaar, J.P. Kamerling, J.F.G. Vliegenthart, J. Biol. Chem. 266 (1991) 4237.
[14] K. Yamamoto, T. Tsuji, T. Irimura, T. Osawa, Biochem. J. 195 (1981) 701.
[15] T. Tsuji, K. Yamamoto, T. Irimura, T. Osawa, Biochem. J. 195 (1981) 691.
[16] J. Charlwood, H. Birrell, A. Organ, P. Camilleri, Rapid Commun. Mass Spectrom. 13 (1999) 716.
[17] R.N. Knibbs, I.J. Goldstein, R.M. Ratcliffe, N. Shibuya, J. Biol. Chem. 266 (1991) 83.
[18] D.C. Kilpatrick, M.M. Yeoman, Biochem. J. 175 (1978) 1151.
[19] K. Yokoyama, T. Terao, T. Osawa, Biochem. Biophys. Acta 538 (1978) 384.
[20] R.D. Cummings, S. Kornfeld, J. Biol. Chem. 257 (1982) 11230.
[21] S. Hammarström, M.L. Hammarström, G. Sundblad, J. Arnarp, J. Lönngren, Proc. Natl. Acad. Sci. U.S.A. 79 (1982) 1611.
[22] K. Tazaki, N. Shibuya, Plant Cell Physiol. 30 (1989) 899.
[23] K. Kornfeld, M.L. Reitman, R. Kornfeld, J. Biol. Chem. 256 (1981) 6633.
[24] S. Teneberg, J. Angstrom, P. Jovall, K. Karlsson, J. Biol. Chem. 269 (1994) 8554.
[25] K. Yamamoto, T. Tsuji, I. Matsumoto, T. Osawa, Biochemistry 20 (1981) 5894.
[26] C.F. Brewer, L. Bhattacharyya, J. Biol. Chem. 261 (1986) 7306.
[27] K. Yasmashita, N. Kochibe, T. Ohkura, I. Ueda, A. Kobata, J. Biol. Chem. 260 (1985) 4688.
[28] K. Yamashita, A. Hitoi, A. Kobata, J. Biol. Chem. 258 (1983) 14753.
[29] T. Tai, K. Yamashita, M. Ogata-Arakawa, N. Koide, T. Muramatsu, S. Iwashita, Y. Inoue, A. Kobata, J. Biol. Chem. 250 (1975) 8569.
[30] T. Tai, K. Yamashita, S. Ito, A. Kobata, J. Biol. Chem. 252 (1977) 6687.
[31] M. Nakano, K. Kakehi, M. Tsai, Y.C. Lee, Glycobiology 14 (2004) 431.
[32] X. Wei, C. Dulberger, L. Li, Anal. Chem. 82 (2010) 6329.
[33] W. Weiss, W. Poste, A. Görg, Electrophoresis 12 (1991) 323.
[34] A. Guttman, Nature 380 (1996) 461.
[35] S. Honda, S. Suzuki, T. Nitta, K. Kakehi, J. Chromatogr. 438 (1988) 73.

ANALYTICAL SCIENCES APRIL 2011, VOL. 27

Affinity Entrapment of Oligosaccharides and Glycopeptides Using Free Lectin Solution

Masahiro YODOSHI, Takehiro OYAMA, Ken MASAKI, Kazuaki KAKEHI, Takao HAYAKAWA, and Shigeo SUZUKI†

Faculty of Pharmaceutical Sciences, Kinki University, 3-4-1 Kowakae, Higashi-osaka, Osaka 577-8502, Japan

Two procedures were proposed for the specific recovery of fluorescent derivatives of glycoprotein-derived oligosaccharides and tryptic glycopeptides using certain plant lectins. The first was based on the salting out of oligosaccharide-lectin conjugates with ammonium sulfate. Oligosaccharides specifically bound to lectins were recovered free from lectins using ethanol precipitation after dissolution in water. This method enabled group separation of 2-aminopyridine-labeled oligosaccharides derived from ovalbumin to galacto-oligosaccharides and agalacto-oligosaccharides by *Ricinus communis* agglutinin, and to high mannose- and hybrid-type oligosaccharides by wheat-germ agglutinin. Fractional precipitation based on differences in affinity for concanavalin A was accomplished by adding an appropriate concentration of methyl α-mannoside as an inhibitor. In the second method, tryptic digests of glycoproteins were mixed with a lectin solution, and the glycopeptide-lectin conjugates were specifically trapped on a centrifugal ultrafiltration membrane with cut-off of 10 kD. Trapped glycopeptides, as retentates, were passed through membranes by resuspension in diluted acid. This method is particularly useful for the enrichment of glycopeptides in protease digestion mixtures for glycosylation analyses by liquid chromatography–mass spectrometry.

(Received January 20, 2011; Accepted March 4, 2011; Published April 10, 2011)

Introduction

Lectins are proteins of non-immune origin that interact specifically with carbohydrates without modifying them.[1,2] Several reports have stated that plant lectins bind primarily to monosaccharides,[3] but that they bind to specific sequences of oligosaccharides with higher affinity. For example, concanavalin A (Con A) binds to α-glucoside and α-mannoside with a K_a on the order of 10^3, but a K_a of 10^6 to 10^7 engenders binding to high mannose-type oligosaccharides.[4,5] In addition, the binding capability of lectins might not reflect the structural differences of the oligosaccharides. Therefore, the inhibitory action is dependent only on the concentration of inhibitors and their affinity for the lectins. High specificity of plant lectins against certain oligosaccharides is helpful for profiling in glycoproteomic analyses. Lectin affinity capillary electrophoresis[6,7] and lectin microarray[8] have been proposed for this purpose. Moreover, the combinational use of affinity columns of immobilized lectins is useful in sorting complex mixtures of oligosaccharides based on structural differences.[9] In a typical separation procedure, the bound oligosaccharides are eluted from the lectin affinity columns by the addition of haptenic sugars.[10] More recently, the use of high-performance lectin-affinity enrichment of glycoprotein using a series of silica-bound lectins at microscale levels has been reported.[5,11-13] This enrichment procedure was combined with nano-liquid chromatography–tandem mass spectrometry (nano-LC-MS) to identify numerous glycoproteins.[13] A multi-lectin column prepared by mixing three lectin-immobilized gels was successively used in enrichment of serum glycoproteins.[14] However, despite the high efficiency of the combinational use of lectin-affinity columns, few studies have used that method because it necessitates special care for the preparation and maintenance of affinity columns. Recently, Hong *et al.* proposed ultrafiltration as a convenient tool to trap an affinity complex instead of using affinity columns, and they used the method to identify Cu^{2+}-protein adducts in saliva.[15]

We report on simple methods for the specific recovery of glycoconjugates from complex samples using lectins without immobilization to a support. Because of the strong affinity of lectins to glycoprotein-derived oligosaccharides, the oligosaccharide-lectin complex is highly stable and not dissociated by precipitation using ammonium sulfate. The precipitates were resuspended in water; oligosaccharides specifically bound to a lectin were dissociated by alcoholic denaturation. This method was applied to the specific fractionation of 2-aminopyridine (AP) derivatives of ovalbumin-derived oligosaccharides. Another method was developed for glycopeptide enrichment based on the specific recovery of lectin-oligosaccharide complexes on a centrifugal ultrafiltration membrane with a cut-off of 10 kDa. Glycopeptides specifically trapped on a membrane were recovered by treatment with diluted acid. This method simplified the interpretation of LC/MS data for glycopeptide analyses.

† To whom correspondence should be addressed.
E-mail: suzuki@phar.kindai.ac.jp

Abbreviations: AP, 2-aminopyridine; WGA, wheat germ agglutinin; RCA_{120}, *Ricinus communis* agglutinin; Con A, concanavalin A; SSA, *Sambucus sieboldiana* lectin; MAM, *Maackia amurensis* agglutinin; Gal, D-galactose; GlcNAc, *N*-acetyl D-glucosamine; Man, D-mannose; Fuc, L-fucose; NeuAc, *N*-acetyl neuraminic acid.

Experimental

Chemical and buffers

The lectins used in the present study, Con A, wheat germ agglutinin (WGA), *Ricinus communis* agglutinin (RCA_{120}), *Sambucus sieboldiana* lectin (SSA), and *Maackia amurensis* agglutinin (MAM), were purchased from Seikagaku Corp. (Tokyo, Japan). Ovalbumin was prepared according to a procedure described by Kekwick and Cannan.[16] L-1-Tosylamido-2-phenylethyl chloromethyl ketone (TPCK)-treated trypsin from bovine pancreas (EC 3.4.21.4), bovine pancreas ribonuclease B, human transferrin, and iodoacetamide were obtained from Sigma-Aldrich, Japan K.K. (Tokyo, Japan). Methyl and *p*-nitrophenyl α-D-mannopyranoside, and AP were from Nacalai Tesque Incorporated (Karasuma, Kyoto, Japan). Before use, AP was recrystallized thrice from hexane. AP-labeled oligosaccharides were prepared from ovalbumin, as described previously.[17] Peptide-N^4-(acetyl-β-glucosaminyl)-asparagine amidase (PNGase F, EC 3.2.2.18) was obtained from F. Hoffman La Roche Ltd. (Tokyo, Japan). An ultrafiltration membrane (Ultrafree-MC-10) was obtained from Nihon Millipore Ltd. (Tokyo, Japan). Other reagents and solvents were of the highest grade commercially available.

Procedures for specific recovery

Entrapping methods were optimized based on the affinity between *p*-nitrophenyl α-mannoside and Con A. The amounts bound to Con A were determined using capillary electrophoresis with HP ^{3D}CE® equipment (Agilent Technologies, Santa Clara, USA) using a fused-silica capillary (50 μm i.d., 60 cm) and 100 mM sodium borate buffer (pH 10.0) as the background electrolyte.

Method A: Saccharide samples (≈2 nmol, or oligosaccharides derived from 2 μg of ovalbumin) were dissolved in 10 μL of 50 mM Tris-HCl (pH 7.0) containing 150 mM NaCl, 1 mM $CaCl_2$ and 1 mM $MgCl_2$ (TBS) and mixed with a lectin solution (0.5 mg in 20 μL of TBS) in an ice bath. The solution was allowed to stand for 2 min, and was then mixed with 100 μL of a saturated aqueous solution of ammonium sulfate. The suspended solution was centrifuged at 5000 rpm for 2 min at 4°C. The supernatant was removed; the precipitate was washed by resuspension in saturated ammonium sulfate, and then centrifuged at 5000 rpm for 2 min at 4°C, with removal of the supernatant in the same manner. Precipitated residues were dissolved in 10 μL of water. Lectin was then removed from the reaction mixture by centrifugation at 10000 rpm for 2 min at 4°C, followed by mixing with 40 μL of ethanol. The supernatant was evaporated to dryness and stored at 4°C until use.

Method B: The sample solution (5 μg dissolved in 10 μL of TBS) was mixed with a lectin solution (0.5 mg in 20 μL of TBS) in an ice bath and allowed to stand for 2 min. The lectin complexation solution was poured onto a centrifugal ultrafiltration tube (10 kDa). The solution that had passed through was discarded after centrifugation at 10000 rpm for 10 min. The retentate was mixed with 100 μL of 10 mM HCl. Glycoconjugates dissociated from a lectin were recovered as a filtration solution by centrifugation (10000 rpm for 10 min). The obtained solution was dried and stored at 4°C.

Analyses of AP-labeled ovalbumin-derived oligosaccharides

The AP-labeled oligosaccharides prepared from 50 μg of ovalbumin were dissolved in 500 μL of water. A 20-μL portion was separated using high-performance liquid chromatography (HPLC) with a gradient HPLC system built of two 870 pumps and an FP-2020plus fluorescence monitor with a flow cell with a volume of 10 μL (Jasco Incorporation, Tokyo, Japan). Data were collected by SmartChrom software (KYA Technologies Corporation, Tokyo, Japan). Labeled oligosaccharides were separated on a reversed-phase column (C_{18}, 5 μm, 6 mm i.d., 15 cm; Nacalai Tesque Incorporation, Kyoto, Japan) with a linear gradient of 0.1 - 0.425% *n*-butanol in 100 mM triethylammonium acetate (pH 4.0) for 100 min at a flow rate of 1.0 mL/min. Fluorometric detection of the analytes was accomplished at an excitation wavelength of 321 nm and an emission wavelength of 383 nm.

LC-MS analyses of tryptic glycopeptides

Tryptic digestion was carried out according to the manufacturer's protocol. Liquid chromatography/electrospray ionization-mass spectrometry (LC/ESI-MS) analyses were conducted using ultra-performance liquid chromatography (UPLC; Prominence series; Shimadzu Corp., Kyoto, Japan) coupled to quadruple ion trap-time of flight (QIT-TOF) equipment (Shimadzu Corp.). Tryptic digests were separated on a reversed-phase column (15 cm × 2.1 mm i.d., HiQsil C18-3; KYA Technologies Corp.) at a flow rate of 0.15 mL/min using gradient elution. The gradient program was 0.1% trifluoroacetic acid (TFA; eluent A) and 60% (v/v) acetonitrile in 0.1% TFA (eluent B); 5 - 5% B at 0 - 2 min, 5 - 60% B at 2 - 42 min, and 60 - 95% B at 42 - 52 min. The eluate from the column was introduced to an orthogonal electrospray interface of a QIT-TOF mass spectrometer with argon gas for ion cooling and collision-induced dissociation (CID) experiments. The QIT-TOF-MS was operated in the positive-ion mode with the probe voltage set to 4.5 kV, a detector voltage of –1.7 kV, a capillary temperature of 200°C, and a nebulizer gas flow of 1.5 L/min. Mass spectra were acquired over the scan range of *m/z* 500 - 2000 with a scan rate of 5 s/scan. The obtained extracted ion chromatograph (EIC) and MS data were processed using LCMSsolution software (Shimadzu Corp.).

Results and Discussion

We proposed two procedures for the specific extraction of glycoconjugates (Fig. 1). In method A, a lectin solution was mixed with a saccharide sample. Lectin-saccharide complexes were salted out by adding ammonium sulfate. The precipitate was dissolved in water, and trapped saccharides freed from lectins by adding ethanol. In method B, a lectin solution was mixed with a saccharide sample, and the mixture passed through an ultrafiltration membrane for a cut-off of 10 kDa by centrifugation. Substances unbound to the lectin were removed in this process. Saccharides residing as lectin complexes on the ultrafiltration membrane were recovered as filtrate by centrifugation after mixing the retentates with acid solution.

Method A was optimized by tuning two factors: (i) the amounts or molar ratio of the saccharide specimen and the lectin in the reaction solution; and (ii) the volume of a saturated solution of ammonium sulfate added to precipitate the complex of the lectin with an oligosaccharide. We chose *p*-nitrophenyl α-mannoside and Con A as model systems to optimize the factors. Con A is most commonly used for the affinity chromatography of oligosaccharides; the K_a value for *p*-nitrophenyl α-mannoside is reportedly 7200 M^{-1}.[5] Results showed that a sample containing <2 nmol of saccharides was quantitatively recovered by adding 0.5 mg of lectin and 100 μL of a saturated ammonium sulfate solution.

In method B, the recovery of mannoside was dependent only

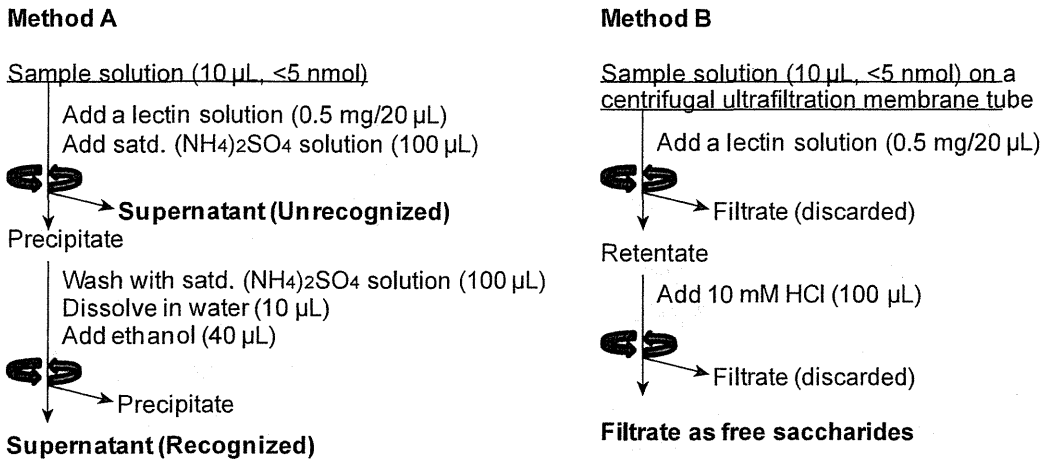

Fig. 1 Procedure for the fractionation of glycans using ammonium sulfate fractionation (method A) and a centrifugal ultrafiltration membrane (method B). TBS: 50 mM Tris-HCl (pH 7.0) containing 150 mM sodium chloride, 1 mM $CaCl_2$ and 1 mM $MgCl_2$. Lectin was dissolved in TBS to a concentration of 25 mg/mL.

upon its molar ratio to Con A. When 0.5 mg of Con A dissolved in 20 μL of buffer was mixed with 10 μL of *p*-nitrophenyl α-mannoside at various concentrations, the recovery decreased linearly, concomitantly with the increase in the mannoside concentration. The recovery ratio changed from >95% for 0.2 nmol of mannoside to 45% for 5 nmol of mannoside. The recovery ratio of 90% obtained using 1 nmol of mannoside seemed to be sufficient for trapping glycoprotein-derived oligosaccharides because their affinity should exceed 10^5 M^{-1}.

Application of method A for specific extraction of ovalbumin-derived oligosaccharides

Method A was applied to the specific recovery of AP-labeled oligosaccharides derived from ovalbumin. The oligosaccharide structures are presented in Table 1. This glycoprotein contains three high mannose-type, one complex-type, and five bisected hybrid-type oligosaccharides, two of which contain one Gal residue. The AP derivatives of these oligosaccharides indicated good resolution in reversed-phase HPLC, which could resolve all except one pair of oligosaccharides (G_1 and G_2) (bottom trace of Fig. 2).[18] We examined method A for the fractionation and recovery of these oligosaccharides using three lectins: RCA_{120}, WGA and Con A.

Figure 2 shows the results of fractions obtained using RCA_{120} and WGA lectins. Ammonium sulfate precipitates as RCA_{120} complexes comprised two components corresponding to peaks G_1 and I (Fig. 2(a)), both of which contained Gal. The supernatant included the remainder of the oligosaccharides (peaks A - F, and H) (Fig. 2(b)). A small peak assignable to G in the supernatant indicated the presence of the Gal-free oligosaccharide G_2. Consequently, RCA_{120} showed an affinity for the Gal-containing hybrid-type oligosaccharide (G_1 and I). The same strategy was also used on the GlcNAc-specific lectin WGA. As depicted in Figs. 2(c) and (d), peaks D - I were inferred to indicate WGA precipitates; peaks A - C corresponding to high mannose-type oligosaccharides were not recognized by WGA, and were recovered as a supernatant fraction. In this chromatogram, some of the recovered peaks indicated apparently reduced intensities, which may be due to a loss in the step of denaturation with ethanol (*i.e.* unspecific coprecipitation with lectin). All *N*-linked oligosaccharides contained a chitobiose core (GlcNAcβ1-4GlcNAc) in their reducing termini, but terminal GlcNAc residues were transformed to linear aminoalditol derivatives by labeling with AP (which impaired their binding capability to WGA). These results indicated that WGA specifically recognized bisecting GlcNAc residues commonly existing in these hybrid-type oligosaccharides. These results showed that RCA_{120} and WGA recognized oligosaccharides having terminal Gal and GlcNAc residues, respectively. Both lectins, therefore, have direct usefulness for the discrimination of hybrid-type oligosaccharides. The results

Table 1 Oligosaccharide derived from ovalbumin and binding specificities to lectins

Peak No.	Structure	Affinity to		
		RCA_{120}	WGA	Con A
A		–	–	++
B		–	–	++
C		–	–	++
D		–	+	++
E		–	+	+
F		–	+	++
G_1		+	+	++
G_2		–	+	+
H		–	+	±
I		+	+	±

Gal ○, Man ○, GlcNAc □,  α-linkage —, β-linkage ▬

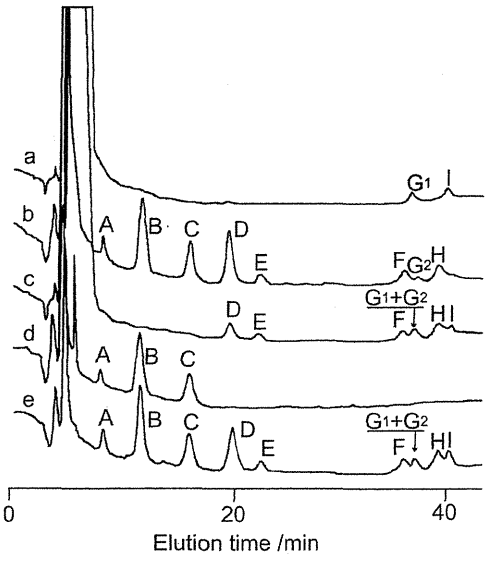

Fig. 2 Analysis of AP-labeled glycans from ovalbumin (e), and their fractions, as retained and unretained as RCA_{120} complex (a, b) and those as WGA complex (c, d). Analytical conditions: Cosmosil C18 (15 cm × 6 mm i.d.) column, 1.0 ml/min flow rate, 100 mM triethylamine/acetic acid (pH 4.0) with a linear gradient of *n*-buthanol (0.1 - 0.425% over 100 min) used as the eluent. Peak identification is presented in Table 1.

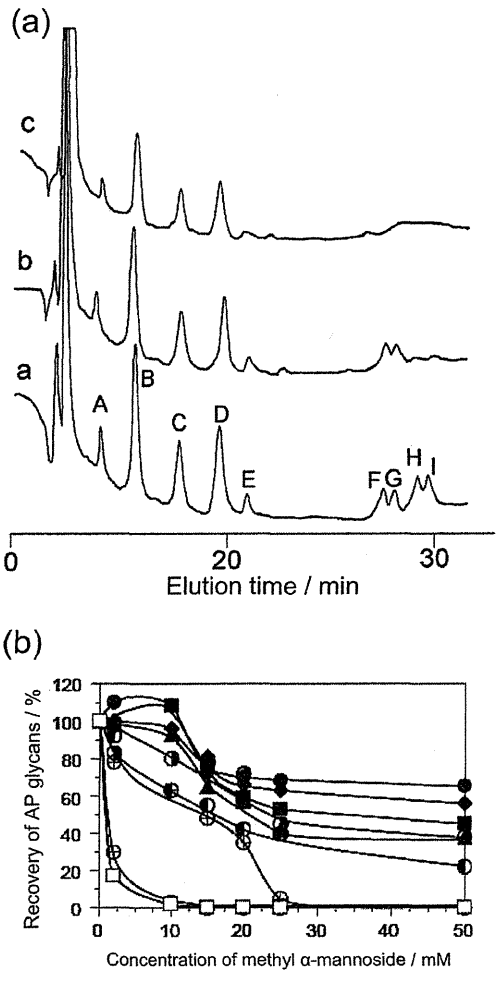

Fig. 3 Analysis of AP-labeled glycans from ovalbumin recovered as Con A complex in the presence of 0 mM (a), 20 mM (b), and 50 mM (c) of methyl α-mannoside (a) and effect of the recoveries of AP-labeled glycans under the presence of methyl α-mannoside (b). The peak assignment and analytical conditions are identical to those in Fig. 2. Symbols: A, ●; B, ■; C, ▲; D, ◆; E, ⊕; F, ◑; G, ◐; H, ⊖; I, □.

underscored the usefulness of the free-lectins strategy for the specific recovery of oligosaccharides with high recovery.

In contrast to WGA and RCA_{120}, Con A seemed to have affinity for all oligosaccharides derived from ovalbumin, and all saccharides were recovered as a Con A complex (Fig. 3). Con A is known to recognize oligosaccharides containing two mannose residues having free hydroxyl groups at their C-3, C-4, and C-6 positions. Actually, Con A shows weak affinity for biantennary oligosaccharides. The interaction between Con A and high mannose-type oligosaccharides can be classified into two groups. Affinity for high mannose-type oligosaccharides containing >7 mannose residues indicates strong binding (K_a $>10^7$ M^{-1}); these binding constants are one order of magnitude higher than that of high mannose-type oligosaccharides containing <6 mannose residues ($K_a \approx 10^6$ M^{-1}).[4] We evaluated the specific recovery of a series of high mannose-type and hybrid-type oligosaccharides based on the difference of affinity for Con A by precipitating the complex of AP-oligosaccharides and Con A in the presence of methyl α-mannoside of various concentrations (Fig. 3). The binding constant of methyl α-mannoside for Con A has been reported to be 7200 M^{-1},[5] which is lower than that of biantennary complex-type oligosaccharides. All ovalbumin oligosaccharides were recognized in the absence of mannoside. With increasing concentrations of methyl α-mannoside, some peaks disappeared; peaks H and I disappeared upon the addition of 10 mM methyl α-mannoside, and peak E disappeared upon the addition of 25 mM of methyl α-mannoside, respectively. However, other peaks were trapped by Con A in the presence of 50 mM mannoside.

Though relational plots in Fig. 3 may include some uncertainty, because some peaks indicated more than 100% of recovery, the inhibitory assay using methyl α-mannoside to Con A seems to be useful in estimating their binding strength of oligosaccharides. The peak area or retention behaviors in affinity chromatography correlate directly to the binding constants. However, the binding plots of these oligosaccharide to Con A showed sigmoid curves, which make it impossible to determine binding constants. This is attributable to the large difference in the binding constants of Con A to mannose (10^3 K_a) and glycoprotein-derived oligosaccharides (*ca.* 10^6 K_a).

Application of method B for the enrichment of tryptic glycopeptides

Method B was applied to LC-MS analyses of glycopeptides in digestion mixtures. Ribonuclease B from bovine pancreas contains a series of high mannose-type oligosaccharides at a single glycosylation site at Asn^{60}.[19] Trypsin predominantly cleaves peptide chains at the carboxyl side of the amino acids of lysine or arginine. Therefore, this glycoprotein is estimated to be digested to >15 species of peptides. Tryptic digestion indicated numerous peaks in the total ion current (TIC) spectra obtained on reversed-phase LC/MS in the positive ion mode (Fig. 4(a)). The sample was treated with Con A, and the retentates recovered and analyzed under the conditions depicted

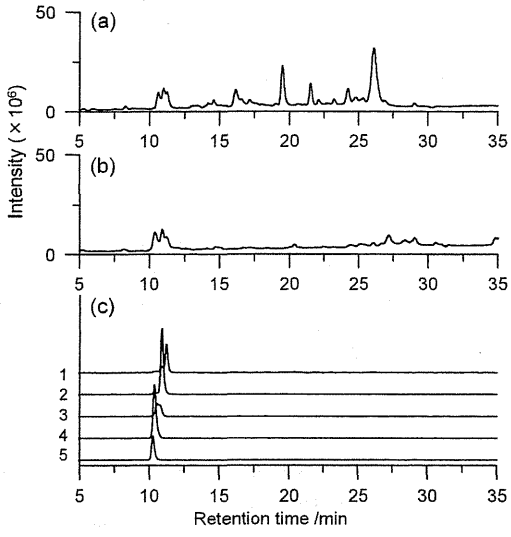

No.	measured m/z	z	glycosylation site	glycan structure with identification based on m/z
1	845.86	2		$[Hex]_5[HexNAc]_2$
2	926.89	2		$[Hex]_6[HexNAc]_2$
3	1079.92	2	Asn^{60}	$[Hex]_7[HexNAc]_2$
4	1089.94	2		$[Hex]_8[HexNAc]_2$
5	1169.97	2		$[Hex]_9[HexNAc]_2$

Fig. 4 Total ion current chromatograms of reversed-phase LC/ESI-MS analysis of glycopeptides derived from bovine ribonuclease B digested with trypsin before (a) and after (b) specific extraction with Con A. Extracted ion chromatograms (c) correspond to trivalent molecular ions of glycopeptides with specific sequences listed in the table. Analytical conditions: column, HiQsil C18-3 (15 cm × 2.1 mm i.d.); flow rate, 0.15 mL/min; eluent, water-acetonitrile with the gradient program described in the Experimental section.

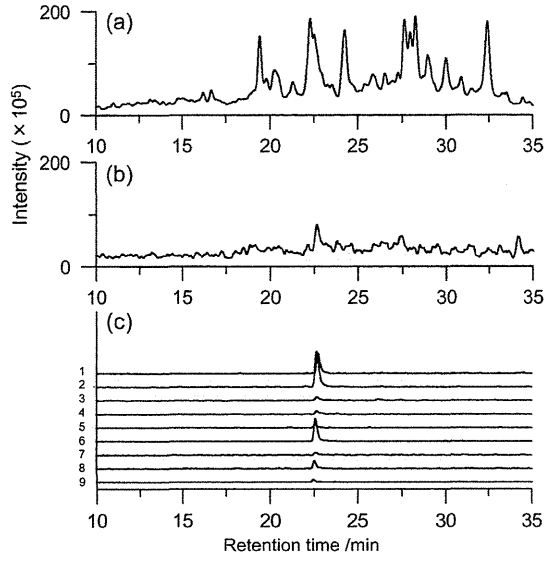

No.	measured m/z	z	glycosylation site	glycan structure with identification based on m/z
1	1542.34	3		$[Hex]_5[HexNAc]_2$
2	1596.34	3		$[Hex]_6[HexNAc]_2$
3	1610.20	3		$[Hex]_5[HexNAc]_3$
4	1625.68	3		$[Hex]_4[HexNAc]_4$
5	1650.35	3	Asn^{293}	$[Hex]_7[HexNAc]_2$
6	1677.68	3		$[Hex]_5[HexNAc]_4$
7	1691.35	3		$[Hex]_4[HexNAc]_5$
8	1745.35	3		$[Hex]_5[HexNAc]_5$
9	1799.35	3		$[Hex]_6[HexNAc]_5$

Fig. 5 Total ion current chromatograms of the reversed-phase LC/ESI-MS analysis of glycopeptides derived from ovalbumin digested with trypsin before (a) and after (b) specific extraction with Con A. Extracted ion chromatograms (c) correspond to trivalent molecular ions of glycopeptides with specific sequences listed in the table. Other conditions are identical to those for Fig. 4.

in Fig. 4(b). Intense peaks were observed at 10 - 12 min. The extracted ion chromatogram (EIC) of each peak clearly indicated that these peaks corresponded to glycopeptides with a specific length of high mannose-type oligosaccharides with a common peptide sequence of NLTK. Their elution order matched that of the decrease in mannose residues. Recoveries of these glycopeptides were 80 - 90% from a comparison of the peak areas. The recoveries were sufficiently good to match those of conventional glycoproteomic studies.

Ovalbumin consists of 385 amino acids with a sequence mass of 43 kDa, and has a single *N*-glycosylation site at Asn^{105}.[20] This glycoprotein therefore contains 33 cleavable sites by trypsin digestion. Figure 5(a) presents a TIC chromatogram of the tryptic digests analyzed using LC/ESI-MS. Retentates as Con A complexes indicated appreciably simple TIC chromatograms (Fig. 5(b)). Furthermore, EIC indicated that glycopeptides bearing a common sequence, YNLTSVLMAMG TTDVFSSSANLSGISSAESLK, were eluted at ≈22.5 min. These glycopeptides were difficult to resolve based on the difference in the oligosaccharide structures. The EIC spectra are portrayed in Fig. 5(c). We could not calculate the recoveries because of insufficient resolution of the glycopeptides. However, the detection of peak 4 corresponding to glycopeptides of oligosaccharide E suggested that the recovery of this method is quantitative because the content of oligosaccharide is less 1% of the total carbohydrate content, the binding constant to Con A is *ca.* 10^3 M^{-1}.

Human serum transferrin has two glycosylation sites at Asn^{432} and Asn^{630}, which bears biantennary complex-type oligosaccharides with two α2,6-linked NeuAc.[21] Therefore, α2,6-linked NeuAc recognizing SSA was chosen to trap transferrin-derived glycopeptides. Because of the higher molecular weight of transferrin (which contains 85 cleavable sites), many peaks were observed on TIC chromatograms (Fig. 6(a)). After extraction with SSA lectin, most peaks disappeared from the chromatogram; the peaks at 20, 22.5, and 24.5 min remained. As shown in EICs, these corresponded to glycopeptides including Asn^{630} and Asn^{432}, respectively. Moreover, we found minor components of Asn^{630} glycopeptides bearing a triantennary oligosaccharide and a fucosylated biantennary oligosaccharide,[22] which was not observed in LC/MS analyses of the original tryptic digests of this glycoprotein. We also applied this method to other lectins, such as *Maackia amurensis* lectin (MAM) specific for α2-3-linked NeuAc. The extract indicated no peaks (data not shown), as expected from its specificity. Although some unidentified peaks were observed at 26 - 30 min on TIC chromatograms of the extract, this method appeared to be useful for the analyses of glycopeptides in tryptic digests of glycoproteins.

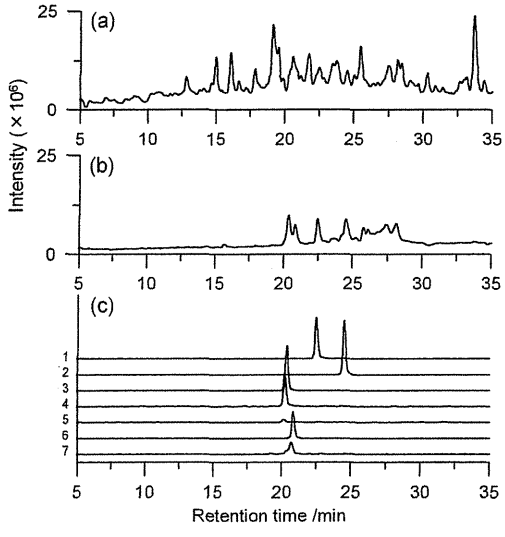

No.	measured m/z	z	glycosylation site	glycan structure with identification based on m/z	peptide mod*1
1	1227.18	3	Asn^{432}	$[Hex]_5[HexNAc]_4[NeuAc]_2$	
2	1222.55	3		$[Hex]_5[HexNAc]_4[NeuAc]_2$	PyroCMC*2
3	1382.28	3		$[Hex]_5[HexNAc]_4[NeuAc]_2$	
4	1430.92	3		$[Hex]_5[HexNAc]_4[dHex][NeuAc]_2$	
5	1503.99	3	Asn^{630}	$[Hex]_6[HexNAc]_5[NeuAc]_2$	
6	1376.59	3		$[Hex]_5[HexNAc]_4[NeuAc]_2$	PyroQ*3
7	1430.92	3		$[Hex]_5[HexNAc]_4[dHex][NeuAc]_2$	PyroQ*3

*1, modification on the peptide moieties; *2, deamination of alkylated cysteine of N-terminus; *3, pyroglutamic acid of N-terminus of peptide

Fig. 6 Total ion-current chromatograms of the reversed-phase LC/ESI-MS analysis of glycopeptides derived from human transferrin digested with trypsin before (a) and after (b) specific extraction with SSA. Extracted ion chromatograms (c) correspond to trivalent molecular ions of glycopeptides with specific sequences listed in the table.

Conclusions

Two methods were developed for the specific recovery and enrichment of glycoconjugates using free lectin solutions. The AP derivatives of ovalbumin oligosaccharides were fractionated based on their affinity for lectins. RCA_{120} enabled the fractionation of galacto-oligosaccharides from agalacto-oligosaccharides, and WGA enabled fractionation of bisected hybrid-type oligosaccharides from high mannose-type oligosaccharides. Complexation with Con A in the presence of methyl α-mannoside also enabled the discrimination of oligosaccharides based on the number of mannose residues in their non-reducing end. Lectin complexation on an ultrafiltration membrane enabled the enrichment of glycopeptides for LC/MS analyses. In addition, Con A affinity was useful for the enrichment of glycopeptides derived from ribonuclease B and ovalbumin. Moreover, SSA enabled the enrichment of NeuAc-containing glycopeptides in tryptic transferrin. These methods yielded results that were comparable with those obtained using affinity chromatography with plant lectins.

Acknowledgements

This work was supported by the "High-Tech Research Center" Project for Private Universities: a matching fund subsidy from the Ministry of Education, Culture, Sports, Science and Technology (MEXT), Japan, 2007.

References

1. I. J. Goldstein, R. C. Hughes, M. Monsigny, T. Osawa, and N. Sharon, *Nature*, **1980**, *285*, 66.
2. O. Mäkelä, *Ann. Med. Exp. Biol. Fenn.*, **1957**, *26*, 11.
3. N. Sharon, *J. Biol. Chem.*, **2007**, *282*, 2753.
4. T. Mega, H. Oku, and S. Hase, *J. Biochem.* [Tokyo], **1992**, *111*, 396.
5. S. Honda, S. Suzuki, T. Nitta, and K. Kakehi, *J. Chromatogr.*, **1988**, *438*, 73.
6. K. Nakajima, M. Kinoshita, Y. Oda, T. Masuko, M. Kaku, N. Shibuya, and K. Kakehi, *Glycobiology*, **2004**, 14.
7. K. Nakajima, Y. Oda, M. Kinoshita, and K. Kakehi, *J. Proteome Res.*, **2003**, *2*, 81.
8. J. Hirabayashi, *J. Biochem.* [Tokyo], **2008**, *144*, 139.
9. R. D. Cummings and S. Kornfeld, *J. Biol. Chem.*, **1982**, *257*, 11235.
10. E. D. Green, R. M. Brodbeck, and J. U. Baenziger, *J. Biol. Chem.*, **1987**, *262*, 12030.
11. M. Madera, Y. Mechref, and M. V. Novotny, *Anal. Chem.*, **2005**, *77*, 4081.
12. L. F. Fraguas, J. Carlsson, and M. Lönnberg, *J. Chromatogr., A*, **2008**, *1212*, 82.
13. A. Monzo, G. K. Bonn, and A. Guttman, *Trends Anal. Chem.*, **2007**, *26*, 423.
14. Z. Yang and W. S. Hancock, *J. Chromatogr., A*, **2004**, *1053*, 79.
15. J. H. Hong, S. E. Duncan, S. F. O'Keefe, and A. M. Dietrich, *Food Chem.*, **2009**, *113*, 180.
16. A. Kekwick and R. K. Cannan, *Biochem. J.*, **1936**, *30*, 227.
17. S. Suzuki, K. Kakehi, and S. Honda, *Anal. Biochem.*, **1992**, *205*, 227.
18. H. Nakagawa, Y. Kawamura, K. Kato, I. Shimada, Y. Arata, and N. Takahashi, *Anal. Biochem.*, **1995**, *226*, 130.
19. T. H. Plummer and C. H. W. Hirs, *J. Biol. Chem.*, **1964**, *239*, 2530.
20. R. D. Palmiter, J. Gagnon, and K. A. Walsh, *Proc. Natl. Acad. Sci. U. S. A.*, **1978**, *75*, 94.
21. M. G. C. M. P. Team, *Proc. Natl. Sci. U. S. A.*, **2002**, *99*, 16899.
22. Y. Satomi, Y. Shimonishi, T. Hase, and T. Takao, *Rapid Commun. Mass Spectrom.*, **2004**, *18*, 2983.

Published OnlineFirst February 23, 2011; DOI:10.1158/1078-0432.CCR-10-2008

Clinical Cancer Research

Enhanced Safety Profiles of the Telomerase-Specific Replication- Competent Adenovirus by Incorporation of Normal Cell-Specific microRNA-Targeted Sequences

Kumiko Sugio, Fuminori Sakurai, Kazufumi Katayama, et al.

Clin Cancer Res 2011;17:2807-2818. Published OnlineFirst February 23, 2011.